

SANDIA REPORT

SAND2021-3389

Printed March 2021

Sandia
National
Laboratories

Fuels Characterization for National Research Council Canada 2-m Pool Fire Test Series

David L. Lord; Joseph W. Hogge; Raymond G. Allen

Prepared by
Sandia National Laboratories
Albuquerque, New Mexico
87185 and Livermore,
California 94550

Issued by Sandia National Laboratories, operated for the United States Department of Energy by National Technology & Engineering Solutions of Sandia, LLC.

NOTICE: This report was prepared as an account of work sponsored by an agency of the United States Government. Neither the United States Government, nor any agency thereof, nor any of their employees, nor any of their contractors, subcontractors, or their employees, make any warranty, express or implied, or assume any legal liability or responsibility for the accuracy, completeness, or usefulness of any information, apparatus, product, or process disclosed, or represent that its use would not infringe privately owned rights. Reference herein to any specific commercial product, process, or service by trade name, trademark, manufacturer, or otherwise, does not necessarily constitute or imply its endorsement, recommendation, or favoring by the United States Government, any agency thereof, or any of their contractors or subcontractors. The views and opinions expressed herein do not necessarily state or reflect those of the United States Government, any agency thereof, or any of their contractors.

Printed in the United States of America. This report has been reproduced directly from the best available copy.

Available to DOE and DOE contractors from

U.S. Department of Energy
Office of Scientific and Technical Information
P.O. Box 62
Oak Ridge, TN 37831

Telephone: (865) 576-8401
Facsimile: (865) 576-5728
E-Mail: reports@osti.gov
Online ordering: <http://www.osti.gov/scitech>

Available to the public from

U.S. Department of Commerce
National Technical Information Service
5301 Shawnee Rd
Alexandria, VA 22312

Telephone: (800) 553-6847
Facsimile: (703) 605-6900
E-Mail: orders@ntis.gov
Online order: <https://classic.ntis.gov/help/order-methods/>



ABSTRACT

This report provides a detailed analysis of the physical and chemical properties of three liquid hydrocarbon fuels: heptane, Bakken crude, and a diluted bitumen, that were subsequently tested in a series of 2-m pool fire experiments at Sandia National Laboratories for the National Research Council Canada. Properties such as relative density, vapor pressure ($VPCR_x$), composition, and heat of combustion were evaluated. The heptane analysis, with relative density = 0.69 (at 15°C), confirmed that the material tested was consistent with high-purity (>99%) n-heptane. The Bakken crude, with a relative density = 0.81 (at 15°C), exhibited a vapor pressure by $VPCR_{0.2}(37.8^\circ\text{C})$ in the range 120-157 kPa. The dilbit, with a relative density = 0.92 (at 15°C) exhibited a vapor pressure by $VPCR_{0.2}(37.8^\circ\text{C})$ in the range 85-98 kPa. Solids remaining in the test pans after the pool fires were also collected and weighed. No detectable solids were left after the heptane burns. In contrast, the crude oils left some brittle, black solid residue. On average, dilbit pool fires left about 40× more residue by mass than Bakken pool fires for equivalent mass of fuel feed.

ACKNOWLEDGEMENTS

This work was funded by the National Research Council Canada and Transport Canada. Additional oil properties data was made available through sharing agreements between Transport Canada and the U.S. Department of Energy.

The authors would like to thank Louis Ory from Intertek for sampling support, Amanda Prefontaine from InnoTech Alberta for consultation on sample handling and analysis methods, and the Fire Sciences team at Sandia National Laboratories for their help with fuel storage, conditioning, and sampling required to meet the objectives of this research study.

CONTENTS

1. Introduction	11
2. n-Heptane Fuel Properties Characterization	13
2.1. <i>n</i> -Heptane Sampling Methods.....	13
2.2. <i>n</i> -Heptane Analysis Methods	14
3. Bakken Crude Sampling and Analysis Methods.....	15
3.1. Large Oil Sample Acquisition and Tanker Operations.....	15
3.2. Subsampling Schedule.....	15
3.3. Subsampling Methods	16
3.3.1. Sampling Events B1, B2, and B3.....	16
3.3.2. Liquid Phase Subsampling (B4) prior to first Bakken pool fire (Test 2.3).....	17
3.3.3. Liquid Phase Subsample (B6) prior to last Bakken Pool Fire (Test 2.6)	18
3.3.4. Solids Sampling (B5 and B7) after Bakken Pool Fires	19
3.4. Bakken Crude Analysis Methods.....	21
3.4.1. Analysis of Sampling Events B1, B2 and B8	21
3.4.2. Analysis of Sampling Events B4 and B6	21
3.4.2.1. VPCR _x (T) (ASTM D6377-M) Expansion Series.....	22
3.4.2.2. Pressurized Compositional Analysis.....	23
3.4.2.3. Unpressurized Physical Properties Determination.....	23
3.4.3. Equation of State (EOS) Modeling	23
4. Diluted Bitumen Sampling and Analysis Methods	25
4.1. Dilbit Sample Acquisition.....	25
4.2. Subsampling Schedule.....	25
4.3. Subsampling Methods	26
4.3.1. Liquid Phase Subsampling (D2) Prior to First Dilbit Pool Fire (Test 3.1)	26
4.3.2. Liquid Phase Subsampling (D4) prior to Last Dilbit Pool Fire (Test 3.6)	28
4.3.3. Solid phase subsampling (D3) after the first Dilbit Pool Fire (Test 3.1).....	29
4.3.4. Solids sampling (D5) after the last Dilbit Pool Fire (Test 3.6).....	31
4.4. Dilbit Crude Analysis Methods	31
4.4.1. Analysis of Sampling Events D1, D2, D4.....	31
5. Experimental Results	33
5.1. General statement on fuels comparison.....	33
5.1.1. Fuel Visual Properties.....	33
5.2. <i>n</i> -Heptane Analysis Results	34
5.3. Crude Oil Unpressurized Properties.....	35
5.3.1. Bakken Physical Properties (Sampling Event B1 – Loading Site)	35
5.4. Fuel Compositions.....	36
5.4.1. Bakken Whole Oil Composition.....	36
5.4.2. Dilbit Whole Oil Composition	39
5.5. Fuel Vapor Pressures	42
5.5.1. Bakken VPCR _x (37.8°C; 100°F) Results.....	42
5.5.2. Bakken VPCR _x (50°C; 122°F) Results.....	43
5.5.3. Dilbit VPCR _x (37.8°C; 100°F) Results.....	44
5.5.4. Dilbit VPCR _x (122°F; 50°C) Results.....	45
5.5.5. Equation of State-Modeled VPCR _x (T)	46
5.6. Other Selected Properties.....	50

5.6.1. Other Bakken Properties	50
5.6.2. Other Dilbit Properties	51
6. Additional Observations	53
6.1. Comparison of Bakken and Dilbit Properties	53
6.2. Diluent Composition in the Dilbit.....	53
6.3. Boiling Point Distributions of the Fuels	55
6.4. Density vs. VPCR	56
6.5. Post-Burn Solids Mass	60
6.5.1. Bakken Residue	60
6.5.2. Dilbit residue.....	61
7. Summary.....	63
8. References	65
Appendix A. Dilbit Tank Fill Data	68
Appendix B. Tabular Listing of VPCR _x Data	69
B.1. Bakken VPCR _x Data.....	69
B.1.1. Direct measurements taken at 37.8 °C and 50 °C.....	69
B.1.2. Summary of measurements on shared Bakken samples from Luketa, Blanchat et al. (2019)	70
B.1.3. Values calculated from process simulator	70
B.2. Dilbit VPCR _x Data.....	71
B.2.1. Direct measurements taken at 37.8 and 50°C.....	71
B.2.2. Values calculated from process simulator	72
Appendix C. Tabular Listing of Compositional Data.....	73
C.1. <i>n</i> -Heptane Compositional Data	73
C.2. Bakken Compositional Data and Whole Oil Properties.....	75
C.3. Dilbit Compositional Data and Whole Oil Properties.....	77

LIST OF FIGURES

Figure 2-1. Photo of the manual drum pump (drum thief sampler) used to transfer heptane from the drums to the glass bottles.	13
Figure 2-2. Photo of heptane source drum (green barrel) and sampling bottles (clear glass, three shown) used here.	14
Figure 3-1. Sandia custom pressurized oil tanker (right) taking a load of crude while displacing water to vacuum truck (left)	15
Figure 3-2. Photo of a 1-L capacity piston cylinder (in shipping case) used to collect pressurized crude oil during Sampling Event B4.....	17
Figure 3-3. Conceptual drawing of tanker recirculation loop and sampling valve.....	17
Figure 3-4. Photos taken during Sampling Event B6 (Burn Site Subsampling 3) at the Sandia thermal test complex on January 31, 2018, prior to the sixth and final 2-m pool fire. Left photo shows a 500-mL capacity floating piston cylinder during oil fill. Right photo shows a “Boston Round” glass bottle containing about 700 mL Bakken crude.	18
Figure 3-5. Photo of transfer process from 500-mL piston cylinder to 1-L piston cylinder on laboratory benchtop. The sample transfer line was evacuated with a vacuum pump prior to sample transfer and then the sample was pushed from the 500-mL piston cylinder into the 1-L piston cylinder with an inert gas.	19

Figure 3-6. Photos of full pan with two insets taken after the January 19, 2018 pool fire, sampling event B5. Spot samples were taken and sent to an offsite laboratory for analysis.....	20
Figure 3-7. Photo of full pan taken after the January 31, 2018 pool fire (sampling event B7). Spot samples were collected and sent to an offsite laboratory for analysis.....	21
Figure 4-1. Photo of eight of the ten modified propane cylinders sent to Sandia to supply the dilbit pool fire testing.....	25
Figure 4-2. Schematic of recirculation loop (a) (reproduced from Prefontaine (2018)) and photo of actual setup.....	27
Figure 4-3. Schematic of combined recirculation/sampling loop reproduced from Prefontaine (2018).....	27
Figure 4-4. Photo of unpressurized glass bottle during ASTM D4057 fill process with dilbit from Tank 12.....	28
Figure 4-5. Photo of pressurized piston cylinder fill process with dilbit from Tank 9. Oil feed on the far end of the cylinder moves the internal piston while displacing glycol through the outlet valve from the close end. The volume of glycol displaced is a primary indicator of sample volume captured in the cylinder.....	29
Figure 4-6. Photo of post-burn solids remaining after Test 3.1. Total mass of solids was measured at 31.48 kg.....	30
Figure 4-7. Close-up photo of sampling post-burn residue from the center of the pan for Test 3.1 on February 7.....	30
Figure 4-8. Photo of post-burn solids remaining after test 3.6. Total mass remaining was measured at 19.60 kg.....	31
Figure 5-1. Comparison of heptane (left), Bakken (center) and diluted bitumen (right) visual properties captured during bottle sampling.....	34
Figure 5-2. Dissolved gas compositions (N ₂ , C1, CO ₂) in Bakken samples taken at loading and at the Sandia burn site.....	37
Figure 5-3. Light ends compositions (C ₂ -nC ₅) in Bakken samples taken at loading and at the Sandia burn site.....	38
Figure 5-4. Whole oil carbon number plots for Bakken oil sampled at loading and burn sites listed by sampling event and replicate number.....	39
Figure 5-5 Dissolved gas contents for the dilbit subsamples at initial subsampling in December and at Sandia's thermal test complex.....	40
Figure 5-6 Light ends (C ₂ -nC ₅) measured for the dilbit subsamples.....	41
Figure 5-7 Whole oil compositions measured for the dilbit subsamples.....	42
Figure 5-8. Pressure-expansion column charts showing measured VPCR _x (100°F; 37.8°C) for the Bakken loading samples (B1) and burn site samples (B2, B4, B6, and B8).....	43
Figure 5-9. Pressure-expansion column charts showing measured VPCR _x (50°C; 122°F) for the Bakken burn site samples (B4 and B6).....	44
Figure 5-10. Pressure-expansion column charts showing measured VPCR _x (37.8°C; 100°F) for the dilbit baseline samples (D1) and burn site samples (D2 and D4).....	45
Figure 5-11. Pressure-expansion column charts showing measured VPCR _x (50°C; 122°F) for the dilbit samples.....	46
Figure 5-12. Column chart comparing measured VPCR _x to EOS-modeled VPCR _x for Bakken loading and burn site samples at T = 100°F; 37.8°C. Measured values are solid bars with 2 σ error bars, modeled values are striped bars.....	47

Figure 5-13 Column chart comparing measured $VPCR_x$ to EOS-modeled $VPCR_x$ for Bakken burn site samples at $T = 50^\circ\text{C}$; 122°F. Measured values are solid bars, modeled values are striped bars.....	48
Figure 5-14. Column chart comparing measured $VPCR_x$ to EOS-modeled $VPCR_x$ for dilbit loading and burn site samples at $T = 37.8^\circ\text{C}$; 100°F. Measured values are solid bars, modeled values are striped bars.	49
Figure 5-15 Column chart comparing measured $VPCR_x$ to EOS-modeled $VPCR_x$ for dilbit samples at $T = 50^\circ\text{C}$; 122°F; Measured values are solid bars, modeled values are striped bars.....	49
Figure 6-1. C4-C14 compositions for the dilbit fuel alongside a condensate and bitumen that were likely used in the stream.	54
Figure 6-2. Measured C4-C14 composition for dilbit fuel (circle, solid line) and a simulated dilbit composition using likely constituents (square, dashed line).....	55
Figure 6-3 Temperature vs. boiling point distribution for the fuels in the burn series	56
Figure 6-4: Overlay of density vs $VPCR_{4}(37.8^\circ\text{C})$ for oils from SPR, PHMSA, NDPC and DOE/DOT/TC COCRS with the fuels tested as part of this project.	57
Figure 6-5: Overlay of density vs. $VPCR_{0.2}(50^\circ\text{C})$ for oils from SPR, COCRS, and TC with the fuels tested as part of this project.....	59

LIST OF TABLES

Table 1-1. High-level test matrix and sampling schedule.....	11
Table 3-1. Listing of sampling events related to overall crude oil project, with NRC/TC sampling indicated in white rows.	16
Table 3-2. Temperature and expansion settings for ASTM D6377 $VPCR_x(T)$ measurements to be run on loading site subsamples.....	22
Table 3-3. Instrument settings for “Equilibrium Time” and “Equilibrium dP/dt ” required to confirm that the analysis run for each V/L has reached equilibrium conditions.	22
Table 4-1. Listing of sampling events supporting the dilbit pool fire series	26
Table 5-1. Summary of average fuel properties observed in this study	33
Table 5-2. Analysis results for composite heptane sample collected from the 9 heptane drums delivered to Sandia.	34
Table 5-3. Physical properties of Bakken samples taken at loading site (B1).	35
Table 5-4. Average measured $VPCR_{0.2}(37.8^\circ\text{C}; 100^\circ\text{F})$ for the five Bakken sampling events.	43
Table 5-5. Average measured $VPCR_{0.2}(37.8^\circ\text{C}; 100^\circ\text{F})$ for the three dilbit sampling events.....	45
Table 5-6. Physical properties of Bakken samples taken at loading site and Sandia burn site.	51
Table 5-7. Physical properties of dilbit samples taken at loading site and Sandia burn site.	52
Table 6-1. A brief comparison of Bakken crude and dilbit properties; bold values represent the larger of the two.	53
Table 6-2: Sources and methods for $VPCR$ and Density data in.....	58
Table 6-3. Sources and methods for $VPCRx(50^\circ\text{C})$ and density data in	60
Table 6-4. Residue mass (kg) and ratio to oil feed (kg/kg) for the 2-m Bakken pool fire series.	61
Table 6-5. Summary of post-burn solids residue recovered from pan.....	62

EXECUTIVE SUMMARY

This report provides a detailed analysis of the physical and chemical properties of three liquid hydrocarbon fuels: high purity n-heptane, Bakken crude, and a diluted bitumen, that were subsequently tested in a series of 2-m pool fire experiments at Sandia National Laboratories for the National Research Council Canada. The results of the pool fire tests are described in a separate report¹. Fuel properties such as relative density, vapor pressure (VPCR_x), composition, and heat of combustion were evaluated. Sampling and analysis methods conformed to published industry standards and were selected based on prior related work, industry best practice, and sponsor request. The heptane analysis, with relative density = 0.69 (at 15°C), confirmed that the range of properties tested were consistent with high-purity (>99%) n-heptane. The Bakken crude, with a relative density = 0.81 (at 15°C), exhibited a vapor pressure by VPCR_{0.2}(37.8°C) in the range 120-157 kPa and composition with peak carbon numbers in the C7-C8 range coupled with a rapidly declining heavy end distribution, terminating in a lumped C25+ in the 5-8 mole% range. The diluted bitumen was the densest fuel tested, with a relative density = 0.92 (at 15°C) and a vapor pressure by VPCR_{0.2}(37.8°C) in the range 85-98 kPa. The composition was characterized by a peak mole% at C5-C6 representing the diluent, overlaid with a long, flat heavy end distribution between C10 and C24 and a lumped C25+ in the 28-30 mole% range. This composition was consistent with a 20-25% mixture by volume of condensate (diluent) with about 75-80 vol% bitumen. Heats of combustion for the three fuels ranged from 43-48 MJ/kg. Solids remaining in the test pans after the pool fires were also collected and weighed. No detectable solids were left after the heptane burns. In contrast, the crude oils left brittle, black solid residue. On average, dilbit pool fires left about 40× more residue by mass than Bakken pool fires for equivalent mass of fuel feed.

¹ Luketa, A., A. Cruz-Cabrera, W. Gill, S. Adey and J. Hogge (2019). "Experimental Results of 2-m Heptane, Bakken Crude Oil, and Dilbit Pool Fire Tests Performed for the National Research Council Canada." *in press*. Sandia National Laboratories, Albuquerque, NM 87185.

ACRONYMS AND DEFINITIONS

Abbreviation	Definition
ANSI	American National Standards Institute
ASTM	ASTM International (standards organization)
BKN	Bakken Crude Oil
CFT	Fort Saskatchewan Condensate
DOE	United States Department of Energy
DOT	United States Department of Transportation
FPC	Floating piston cylinder
GPA	Gas Processors Association
NIST	National Institute of Standards and Technology
NRC	National Research Council Canada
TC	Transport Canada
TDG	Transport of Dangerous Goods
TTC	Thermal Test Complex, Sandia National Laboratories
V/L	Vapor to liquid volume ratio (relevant to ASTM D6377 VPCR testing)
VPCR _x	Vapor pressure of crude oil at vapor-liquid volume ratio "x" by ASTM D6377

1. INTRODUCTION

This report summarizes findings from the sampling and analysis of fuels used for the National Research Council Canada (NRC) 2-m pool fire tests run at the Sandia National Laboratories Thermal Test Complex in Albuquerque, New Mexico, USA. The overarching purpose of the research program is to understand how physical and chemical properties of crude oils affect their combustion properties and hazard potential in the event of an accident involving fire during transportation and handling.

Subsamples of three liquid hydrocarbon fuels: *n*-heptane, Bakken crude oil from North Dakota (API gravity = 42.9, sulfur = 0.1 wt%), and a diluted bitumen (dilbit; API gravity = 21.7, sulfur = 3.6 wt%) from Canada were drawn at Sandia and analyzed at offsite laboratories to monitor selected physical and chemical properties including the composition and vapor pressure (VPCR_x) of the materials at selected times throughout the pool fire test series.

A high-level test matrix is shown below in Table 1-1. The scope of this report covers the fluids and solids sampling in columns 4 and 5. The combustion test descriptions and results related to column 3 are given in a separate report (Luketa, Cruz-Cabrera et al. 2019).

Table 1-1. High-level test matrix and sampling schedule.

1	2	3	4	5
		Pool Fire	Pre-burn	Post-burn
Pool Fire Test #	Fuel	Test Date	Fluids Sampling	Solids Sampling
Test Series 1				
1.1	Heptane	12/6/2017	12/4/2017	-
1.2	Heptane	12/7/2017	-	-
1.3	Heptane	12/8/2017	-	-
Test Series 2				
2.3	Bakken	1/19/2018	1/19/2018	1/22/2018
2.4	Bakken	1/24/2018	-	-
2.5	Bakken	1/25/2018	-	-
2.1	Bakken	1/29/2018	-	-
2.2	Bakken	1/30/2018	-	-
2.6	Bakken	1/31/2018	1/31/2018	2/1/2018
Test Series 3				
3.1	Dilbit	2/6/2019	1/28/2019	2/7/2019
3.2	Dilbit	2/14/2019	-	2/15/2019
3.3	Dilbit	2/20/2019	-	2/21/2019
3.4	Dilbit	2/25/2019	-	2/26/2019
3.5	Dilbit	2/27/2019	-	2/28/2019
3.6	Dilbit	3/4/2019	2/27/2019	3/5/2019

This page left blank

2. N-HEPTANE FUEL PROPERTIES CHARACTERIZATION

In this chapter, heptane sampling and property analyses are described. Heptane was used as combustion fuel in a series of 2-m pool fire tests that preceded the Bakken and dilbit pool fire test series. Heptane pool fire data is useful as baseline liquid fuel data for testing and troubleshooting analytical equipment and comparing with crude oils.

2.1. *n*-Heptane Sampling Methods

The heptane fuel arrived at Sandia from a commercial supplier in nine drums of nominally 50 gallons capacity each. A liquid subsample was taken from each using a drum thief sampler compliant with ASTM D4057 (ASTM 2012), Section 7.14: Tube Sampler--Drum or Barrel. See Figure 2-1 for a photo of the sampler used in this work. A single 500-700 mL sample was pulled from each drum, giving nine samples total. Each of these nine samples was placed into a separate unpressurized clear glass bottle. Figure 2-2 shows a drum and several of these sample bottles. An unpressurized sampling approach for collecting, holding, and transporting heptane samples was deemed acceptable in this work because the relatively low vapor pressure (~ 11 kPa @ 37.8 °C; (Williamham, Taylor et al. 1945)) and uniformity in composition of *n*-heptane minimize risk of loss of light ends and resultant property changes during sampling and handling at ambient conditions.



Figure 2-1. Photo of the manual drum pump (drum thief sampler) used to transfer heptane from the drums to the glass bottles.



Figure 2-2. Photo of heptane source drum (green barrel) and sampling bottles (clear glass, three shown) used here.

The samples were labeled and boxed at Sandia, then shipped offsite for analysis. Once the samples reached the lab, equal volumes from each of the nine bottles were combined to form a composite sample. All analytical test results presented here represent properties of this composite sample.

2.2. *n*-Heptane Analysis Methods

Heptane samples were analyzed for the following properties:

1. Purity by chromatographic method ASTM D6730-M (ASTM 2011b) for heptane
2. Relative Density by ASTM D4052 (ASTM 2011a)
3. Heat of Combustion by ASTM D240 (ASTM 2014)
4. Water Content by ASTM E1064 (ASTM 2016g)
5. Flash Point by ASTM D93A (ASTM 2013b)
 - a. Additional Flash Point by ASTM D3828 (ASTM 2016h) by sponsor request
6. Average Molecular Weight by cryoscope (freezing point depression)

3. BAKKEN CRUDE SAMPLING AND ANALYSIS METHODS

This chapter describes the methodology for sampling and analysis of the Bakken crude oil used in the pool fire test series described in Luketa, Cruz-Cabrera et al. (2019). Six pool fires were run with Bakken crude oil in this study. Sandia monitored and coordinated collection and analysis of the crude oil subsamples to establish basic physical and chemical properties of the fuel.

3.1. Large Oil Sample Acquisition and Tanker Operations

Crude oil was acquired from a terminal in North Dakota that handles Bakken production and placed in a custom-designed pressurized tanker truck. The 4,800-gal pressurized tanker (shown in Figure 3-1) used water displacement to isolate the fuel sample from changes in light ends and fixed gases. This main sample of 2,100 gallons of oil was further sampled at different times to characterize any loss of volatile components during the fire testing and the resulting effect on the testing process. These smaller samples were called “subsamples.” Additional detail on sample acquisition is provided in Luketa, Blanchat et al. (2019).



Figure 3-1. Sandia custom pressurized oil tanker (right) taking a load of crude while displacing water to vacuum truck (left)

3.2. Subsampling Schedule

The tanker load of Bakken crude oil was shared by several sponsoring entities including the U.S. Department of Energy (DOE), U.S. Department of Transportation (DOT), Transport Canada, (TC) and the National Research Council Canada (NRC) during the crude oil characterization research program. To reiterate, the 2,100-gallon tanker-load was considered the main oil sample, while the spot samples taken from the main oil for quality testing were considered subsamples. Overall, eight sampling events were planned, the first three and last of which were conducted under the DOE/DOT/TC project, and the 4th-7th were conducted under the NRC/TC project. The current report describes the sampling and analysis specific to the NRC/TC project, represented by events B4-

B7 in the lower half of Table 3-1. Information about the DOE/DOT/TC sampling and analysis plan (Events B1-B3 and B8, shaded) is given in Luketa, Blanchat et al. (2019).

Table 3-1. Listing of sampling events related to overall crude oil project, with NRC/TC sampling indicated in white rows.

Event #	Fuel	Event Name in Multi-Agency Project Schedule	Sponsor	Description
B1	Bakken	Loading Site Subsampling	DOE/DOT/TC	Fluid sampling taken at the crude oil loading site for oil before it entered the tanker
B2	Bakken	Burn Site Subsample 1	DOE/DOT/TC	Fluid sampling taken at the Sandia burn site after homogenization and just prior to use in the 5m pool fire
B3	Bakken	5-m Pool Fire Solids Residue	DOE/DOT/TC	Post-burn solids collected from the pool fire pan
B4	Bakken	Burn Site Subsample 2	NRC/TC	Fluid sampling taken at the Sandia burn site (Thermal Test Complex) after homogenization and just prior to use in the first 2-m pool fire (Pool Fire Test 2.3)
B5	Bakken	2-m Pool Fire Solids Residue	NRC/TC	Post-burn solids collected from the pool fire pan (Pool Fire Test 2.3)
B6	Bakken	Burn Site Subsample 3	NRC/TC	Fluid sampling taken at the Sandia burn site (Thermal Test Complex) after homogenization and just prior to use in the last 2-m pool fire (Pool Fire Test 2.6)
B7	Bakken	2-m Pool Fire Solids Residue	NRC/TC	Post-burn solids collected from the pool fire pan (Pool Fire Test 2.6)
B8	Bakken	July 2018 Subsample	DOE/DOT/TC	Fluid sampling taken at the Sandia burn site in the month of July 2018

3.3. Subsampling Methods

Enough sample volume was collected at each liquid sampling point (Sampling Events B1, B2, B4, B6, and B8) so that the relevant analytical portion of the analysis plan could be performed twice. As such, half of the samples were utilized in analysis and the other half were retained in reserve for backup analysis if needed.

3.3.1. Sampling Events B1, B2, and B3

Descriptions of subsampling events Loading Site Subsample (B1) and Burn Site Subsample 1 (B2) are given in Luketa, Blanchat et al. (2019). Pool fire solids residue from B3 was acquired and shipped to a lab that was under contract with TC.

3.3.2. Liquid Phase Subsampling (B4) prior to first Bakken pool fire (Test 2.3)

A fluid subsample (B4) was taken from the pressurized tanker at the Sandia Thermal Test Complex (TTC) to establish properties of the material within one day of the first 2-m crude oil pool fire test.

Crude oil samples for vapor pressure and composition were collected using closed cylinder sampling methods displacing a glycol-water mixture, compliant with Gas Processors Association (GPA) standard GPA 2174 (GPA 2014). Source oil pressure was maintained between 40-45 psig to facilitate operation of the piston cylinder devices. Six 1-L capacity piston cylinders (see Figure 3-2) were filled to nominally 700 mL each, displacing a water-glycol mixture as the container was loaded with oil. In addition, six 700 mL samples for unpressurized physical property analysis were obtained by ASTM D4057 in 1-L glass bottles.



Figure 3-2. Photo of a 1-L capacity piston cylinder (in shipping case) used to collect pressurized crude oil during Sampling Event B4.

All the above-mentioned subsamples were pulled from a sampling manifold system attached to a recirculation loop on the pressurized Sandia tanker (see conceptual drawing in Figure 3-3). The tanker contents were circulated for several hours by a dedicated recirculation loop to homogenize the contents prior to subsampling and injection into the fire testing facility. The oil was circulated for enough time to allow at least 3 tanker volumes of oil to pass through the circulation pump.

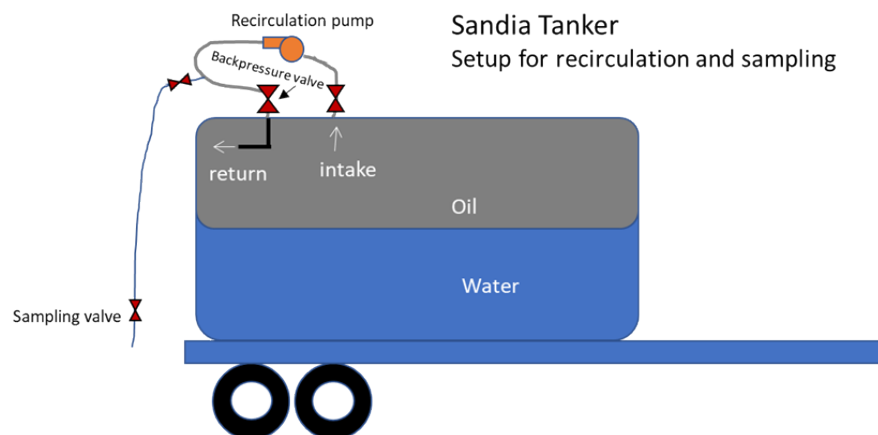


Figure 3-3. Conceptual drawing of tanker recirculation loop and sampling valve.

3.3.3. Liquid Phase Subsample (B6) prior to last Bakken Pool Fire (Test 2.6)

A fluid subsample from Sampling Event B6 (Burn Site Subsample 3) was taken from the pressurized tanker at the Sandia Thermal Test Complex (TTC) to establish properties of the material just prior to the last 2-m crude oil pool fire test (see photos in Figure 3-4).



Figure 3-4. Photos taken during Sampling Event B6 (Burn Site Subsampling 3) at the Sandia thermal test complex on January 31, 2018, prior to the sixth and final 2-m pool fire. Left photo shows a 500-mL capacity floating piston cylinder during oil fill. Right photo shows a “Boston Round” glass bottle containing about 700 mL Bakken crude.

The sampling method varied slightly from prior events because empty 1-L piston cylinders were not available at the Sandia site at the time of sampling. Instead, 500-mL piston cylinders were filled in the field using back-pressure of an inert gas to control the fill rate. The 500-mL piston cylinders were shipped to a crude oil laboratory facility in the US where the samples were transferred to 1-L piston cylinders (see Figure 3-5 for a photo and description of the setup). The 1-L piston cylinders were shipped to their final destination at another crude oil laboratory in Canada where they were analyzed. This transfer of the sample from the 500-mL piston cylinder to a 1-L piston cylinder was required since the 1-L piston cylinders were certified for transport of crude oil samples per Transport Canada regulations. Also, six 700 mL samples for unpressurized physical property analysis were obtained by ASTM D4057 in 1-L glass bottles.

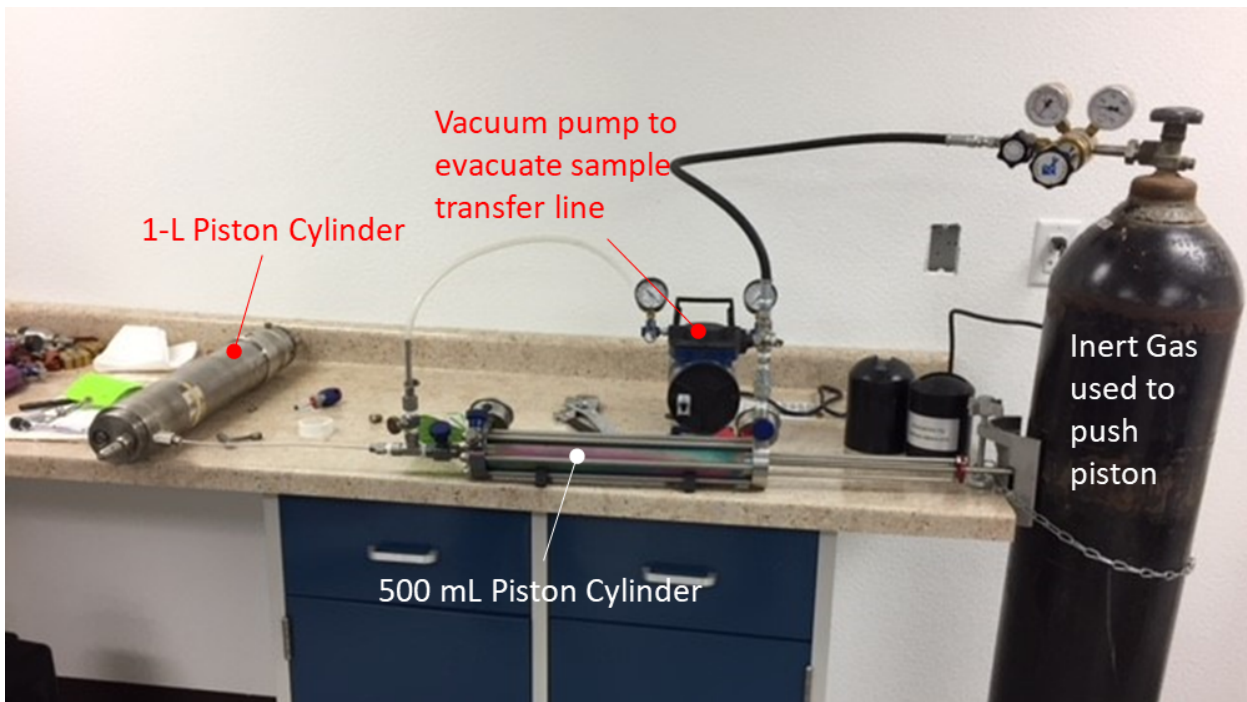


Figure 3-5. Photo of transfer process from 500-mL piston cylinder to 1-L piston cylinder on laboratory benchtop. The sample transfer line was evacuated with a vacuum pump prior to sample transfer and then the sample was pushed from the 500-mL piston cylinder into the 1-L piston cylinder with an inert gas.

3.3.4. Solid Phase Subsampling (B5 and B7) after Bakken Pool Fires

The 2-m Post Burn Solids Residue sample after pool fire test 2.3 (Sampling Event B5) and the 2-m Post Burn Solids Residue after pool fire test 2.6 (Sampling Event B7) were taken to evaluate some basic features of the residue. On-site analyses included:

- Photographs of pan
- Qualitative description of residual material (solid, slurry, viscous liquid or paste)
- Total mass of residual material

Three samples were collected and placed into plastic wide-mouth sampling jars for offsite laboratory analyses that were outside the scope of this report. The three locations for analysis represented the center of the pan, midpoint along the radius of the pan, and the outer edge against the lip of the pan. Sampling procedures were guided by ASTM D4057-12 (ASTM 2012), section 9.29.2: solid and semi-solid grab sampling.

The Bakken post-burn solids were dry and brittle. Deposition quantity and quality did not appear to depend on radius. Photos of the pan residue after the Jan 19 test (Sampling Event B5) and the Jan 31 test (Sampling Event B7), are shown in Figure 3-6 and Figure 3-7, respectively. In areas where solids deposition was thickest, a light gray dusty material appeared to sit on top of a dark black glassy solid that was cemented to the pan.



Figure 3-6. Photos of full pan with two insets taken after the January 19, 2018 pool fire, sampling event B5. Spot samples were taken and sent to an offsite laboratory for analysis.



Figure 3-7. Photo of full pan taken after the January 31, 2018 pool fire (sampling event B7). Spot samples were collected and sent to an offsite laboratory for analysis.

3.4. Bakken Crude Analysis Methods

The analysis methods used on the samples depended on the sample sources. The fluid subsamples taken at tanker loading (Event B1 in Table 3-1) were subjected to a range of physical property tests that provide a general physical description commonly used to evaluate oil quality in the midstream sector. The fluid subsamples taken at the burn site (Events B2, B4, B6, B8 in Table 3-1) were subjected to a more particular set of tests centered around volatility and combustion properties.

3.4.1. Analysis of Sampling Events B1, B2 and B8

Loading Site Subsampling (Sampling Event B1), Burn Site Subsample 1 (Sampling Event B2), Burn Site Subsample 4 (Sampling Event B8) and their analyses were funded and directed under the US DOE/DOT/TC project and are described in Luketa, Blanchat et al. (2019).

3.4.2. Analysis of Sampling Events B4 and B6

Sampling Events B4 and B6 were taken directly before Pool Fire Test 2.3 and 2.6, respectively. As such, detailed analyses were performed on these samples to more directly link the properties of the crude oil to the pool fires. Analysis methods for the fluids collected in Sampling Events B4 and B6 include:

- VPCR_x(T) by ASTM D6377-M (ASTM 2016b) at selected temperature and expansion points listed in Table 3-2
- Pressurized Compositional Analysis by ASTM D8003 (ASTM 2015) + ASTM D7169 (ASTM 2016a) + GOR merge
- Density by ASTM D5002 (ASTM 2013a)
- Flash Point by ASTM D56 (ASTM 2016d) and D3828 (ASTM 2016h)

- Heat of Combustion by ASTM D240 (ASTM 2014)
- Water Content by ASTM D4007 (ASTM 2016f) and D6304 (ASTM 2016c)

Subsamples for ASTM D6377 VPCR, ASTM D8003 pressurized composition, and GOR analyses were drawn from GPA 2174 pressurized cylinders due to their sensitivity to light end losses and requirement for pressurized sample injection. Flashpoint, heat of combustion, and water content samples were drawn from ASTM D4057 bottle samples. These unpressurized measurements did not show sensitivity to sampling method for similar Bakken oil in prior work (Lord, Allen et al. 2017).

3.4.2.1. VPCR_x(T) (ASTM D6377-M) Expansion Series

A vapor pressure “curve” was developed by running a series of pressure-expansion points on oil from the loading subsample. The selected temperature and expansion points are given in Table 3-2.

Table 3-2. Temperature and expansion settings for ASTM D6377 VPCR_x(T) measurements to be run on loading site subsamples.

Temperature		Expansion Ratio (x)					
(°F)	(°C)	V/L	V/L	V/L	V/L	V/L	V/L
100	37.8	0.2	0.5	1.0	1.5	2.0	4.0
122	50	0.2	0.5	1.0	1.5	2.0	4.0

Samples must be allowed to reach an effective equilibrium for each expansion point, with ASTM D6377 instrument equilibration requirements given in Table 3-3. The equilibrium requirements and sample conditioning have been modified for this project, which changes these measurements from “D6377” to “D6377-M” results, as stated in the note below Table 3-3. This analysis was run in duplicate on separate cylinders to demonstrate reproducibility.

Table 3-3. Instrument settings for “Equilibrium Time” and “Equilibrium dP/dt” required to confirm that the analysis run for each V/L has reached equilibrium conditions.

V/L	Minimum Equilibration Time (sec)	Equilibration dP/dt (kPa/min)
0.20	900	0.2
0.50	600	0.15
1.0	600	0.1
1.5	500	0.1
2.0	400	0.1
4.0	300	0.1

Note: The “M” modifier on the ASTM D6377 test method above relates specifically to the equilibrium criteria above in Table 3-3 and the temperature conditioning of the test fluid. Sandia National Laboratories requires that the test fluid be pre-conditioned to the test temperature PRIOR TO PRESSURIZED INJECTION into the sample chamber in the 6377 device, and that the sample injection tubing and pressure regulators (if required) are also maintained at the test temperature. This is done in order to prevent liquid thermal expansion effects from further pressurizing the cell before the expansion sequence starts, leading to erroneously high-pressure values for low V/L.

3.4.2.2. Pressurized Compositional Analysis

Bakken sample compositions on a “whole oil” basis were determined by combining ASTM D8003-15, ASTM D7169, and GOR flash measurements by numerical recombination. Doing so yielded whole oil descriptions with components including N_2+O_2 , CO_2 , carbon number groups including major isomers from C1-C24, and a lumped heavy portion given as C25+. Density of pressurized samples was also measured using ASTM D5002. Mole% and mass% reported in the experimental results are given by component as a percentage of the whole, original sample.

3.4.2.3. Unpressurized Physical Properties Determination

The burn site subsamples were analyzed for the following physical properties using unpressurized sampling and storage techniques. Sample collection (ASTM D4057) and handling were consistent with procedures given in each associated standard.

- Flash Point (ASTM D56 and ASTM D3828)
- Heat of Combustion (ASTM D240)
- Water Content (ASTM D4007 and ASTM D6304)

3.4.3. Equation of State (EOS) Modeling

Bakken crude oils with compositions measured by the pressurized compositional analyses described in Section 3.4.2.2 were simulated via commercially available process simulation software. This simulation used a cubic equation of state (EOS) model embedded in the process simulation software to predict properties such as vapor pressure at selected V/L and temperature based on composition. The compositional data were used to model the oil samples for several reasons:

1. A favorable comparison of modeled properties from the compositionally-based EOS with measured properties from the analytical lab provides a level of verification that the composition and properties of the whole oil are self-consistent and that the EOS model is appropriate for this particular application.
2. Producing modeled VPCR_x from compositional data helps identify which compositional factors in a crude oil affect its VPCR_x, and in what ways.
3. Having access to a validated simulation model can enable predictions of oil properties where direct measurements are not feasible due to expense, difficulty, or safety concerns.

More information on the EOS modeling procedures used here can be found in a previous study (Lord, Allen et al. 2017).

This page left blank

4. DILUTED BITUMEN SAMPLING AND ANALYSIS METHODS

This chapter describes the methodology for sampling and analysis of the diluted bitumen (dilbit) crude oil used in the pool fire test series described in Luketa, Cruz-Cabrera et al. (2019). Six pool fires were run with dilbit crude oil in this study. Sandia monitored and coordinated collection and analysis of crude oil subsamples to establish basic physical and chemical properties of the fuel.

4.1. Dilbit Sample Acquisition

Twelve cylinders of diluted bitumen were acquired by InnoTech Alberta on November 28th and 29th, 2018 from a pipeline source in Canada. The dilbit was contained in 420-lb customized propane tanks, displacing nitrogen during fill. Approximate capacity for these cylinders was 360 L (95 gal), with a tare weight of 130 kg (290 lb). Tank ID's (1-12) were pre-assigned by InnoTech and written directly onto the tank shells. Ten tanks were then shipped to the Sandia facility in Albuquerque, NM USA in December 2018. Two tanks were retained at InnoTech. Once at Sandia, the cylinders were stored outdoors on pallets over secondary spill containment as shown in Figure 4-1.



Figure 4-1. Photo of eight of the ten modified propane cylinders sent to Sandia to supply the dilbit pool fire testing.

4.2. Subsampling Schedule

The dilbit subsampling schedule is summarized below in Table 4-1. Liter-scale loading site subsamples were acquired on November 28-29, 2018 (event D0) while the 420-lb tanks were loaded from the pipeline source. The loading subsamples were collected into floating piston cylinders and Boston Round bottles and held in retention and not analyzed. Baseline spot samples from one of the 12 tanks (tank 5) were then drawn on December 3, 2018 (D1). Additional sampling details are given in Appendix A on a sample-by-sample basis, as reported by InnoTech.

The liquid phase dilbit was sampled twice at Sandia: once (event D2) before the first pool fire and again (D4) before the last pool fire in the testing series. The solid residue that resulted from each 2-m pool fire was also sampled and weighed after each of the six pool fire tests. Two of those solid samples (event D3, D5), from the first and last fires, were packaged and sent to an offsite laboratory for analysis.

Table 4-1. Listing of sampling events supporting the dilbit pool fire series

Event #	Event Name	Description
D0	Loading Site Subsampling	Baseline fluid subsamples taken directly from pipeline source at same time as the 360L samples were collected. These samples were held in retain and not analyzed.
D1	Baseline Subsampling	Fluid sampling taken from Tank #5 to establish initial properties prior to shipping tanks to Sandia.
D2	Burn Site Subsample 1: Tank 12	Fluid sampling taken at the Sandia thermal test complex after homogenization and just prior to use in the first 2-m dilbit pool fire (Pool Fire Test 3.1).
D3	2-m Pool Fire Solids Residue	Post-burn solids collected from the pool fire pan
D4	Burn Site Subsample 2: Tank 9	Fluid sampling taken at the Sandia thermal test complex after homogenization and just prior to use in the final 2-m dilbit pool fire.
D5	2-m Pool Fire Solids Residue	Post-burn solids collected from the pool fire pan (Pool Fire Test 3.6).

4.3. Subsampling Methods

4.3.1. *Liquid Phase Subsampling (D2) Prior to First Dilbit Pool Fire (Test 3.1)*

Tank 12 was selected to supply the first pool fire test (3.1). The tank was fitted with a recirculation system that drew oil up the hanging string and out of the liquid valve, through a pneumatic diaphragm pump, and back into the vapor valve. A schematic of the recirculation loop is shown in Figure 4-2(a) next to a photo of the actual setup in Figure 4-2(b). The tank was recirculated for about 20 minutes at about 10 gallons per minute to assure that several complete volumes were recirculated prior to subsample collection.

Early efforts to mix the oil were met with problems as the centrifugal pump could not move the viscous oil. As a workaround, electrical resistance pad heaters were fixed to the outside of the dilbit tank (see orange pads in Figure 4-2(b)) to heat the oil and decrease viscosity to facilitate flow and mixing since the mixing and sampling were performed outdoors and subjected to winter temperatures near 0-5°C. Also, a pneumatic diaphragm pump was installed to replace the centrifugal pump. In the end, the heaters were never energized because the pneumatic diaphragm pump was able to move the fluid and mix without external heating.

Pressure for subsampling was generated by adding a recirculation/back pressure valve as shown in Figure 4-3, with a tee that fed a sample line fitted with a sampling valve. Pressure at the sampling valve was maintained between 20-40 psig during sampling.

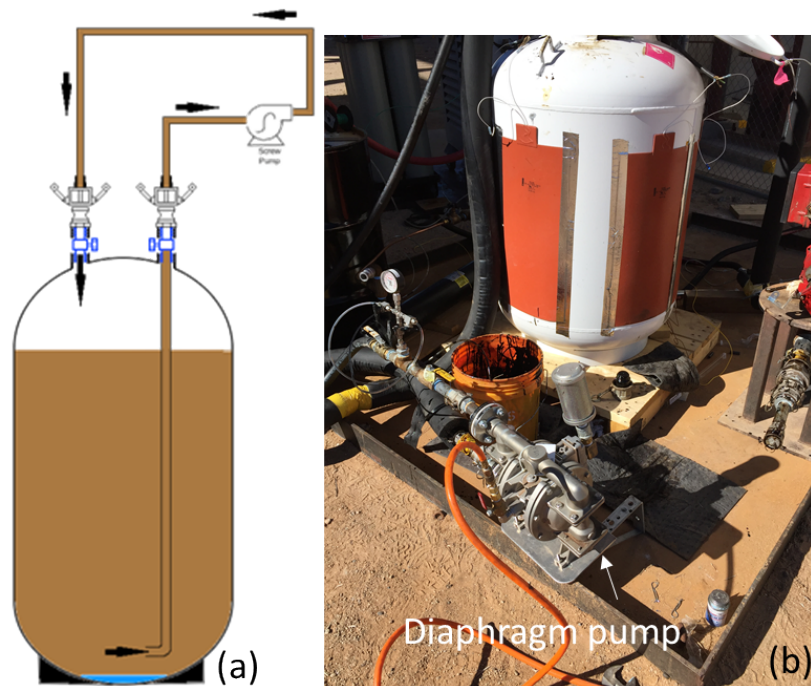


Figure 4-2. Schematic of recirculation loop (a) (reproduced from Prefontaine (2018)) and photo of actual setup.

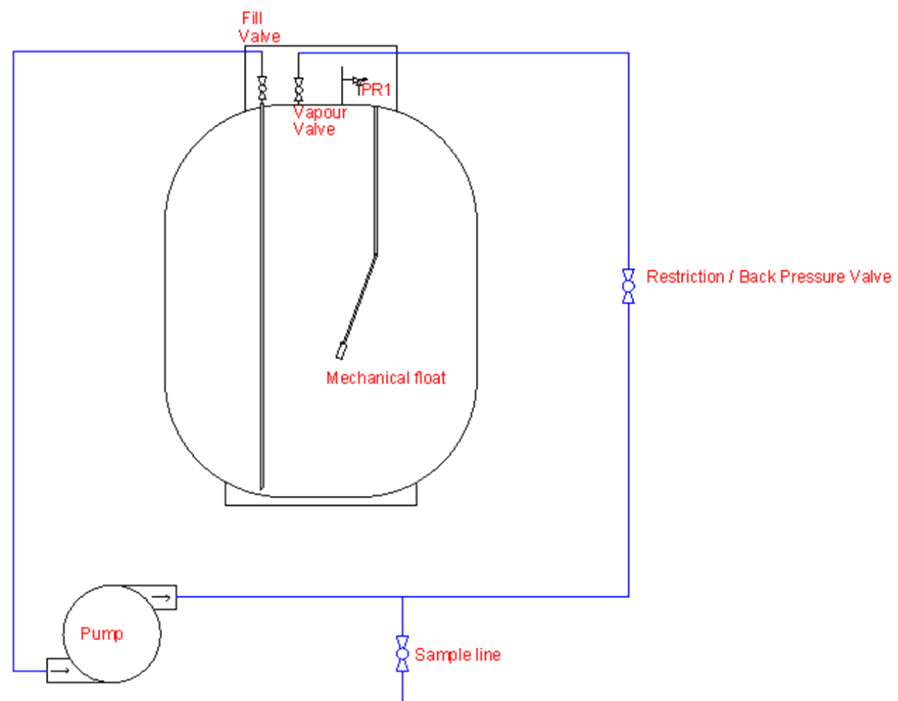


Figure 4-3. Schematic of combined recirculation/sampling loop reproduced from Prefontaine (2018).

Dilbit liquid samples for subsampling event D2 were acquired by two methods:

- GPA 2174-14 pressurized sampling using Proserv 700 mL capacity floating piston cylinders (2 × 700 mL)
- ASTM D4057 unpressurized sampling using Boston round bottles (4 × 700 mL)

The cylinders were received at Sandia already back-filled with glycol. A photo of the unpressurized ASTM D4057 bottle sampling is shown in Figure 4-4. Subsamples were acquired on 1/28/2019 between 1-2 PM local time.



Figure 4-4. Photo of unpressurized glass bottle during ASTM D4057 fill process with dilbit from Tank 12.

4.3.2. *Liquid Phase Subsampling (D4) prior to Last Dilbit Pool Fire (Test 3.6)*

Tank 9 was selected to supply the sixth pool fire test, which was the last in the test series. Oil pre-mixing was performed as described above in section 4.3.1.

Samples were acquired by two methods:

- GPA 2174-14 pressurized sampling using Proserv 700 mL capacity floating piston cylinders (2 × 700 mL)
- ASTM D4057 unpressurized sampling using Boston round bottles (4 × 700 mL)

A photo of the pressurized floating piston cylinder sampling is shown in Figure 4-5. The cylinders were received at Sandia already back-filled with glycol. As oil entered the inlet side of the cylinder, the piston moved to displace glycol at nominally the same volume as oil captured in the cylinder. Subsamples from Tank 9 were collected on 2/27/2019 from 11 AM to 12:20 PM local time.



Figure 4-5. Photo of pressurized piston cylinder fill process with dilbit from Tank 9. Oil feed on the far end of the cylinder moves the internal piston while displacing glycol through the outlet valve from the close end. The volume of glycol displaced is a primary indicator of sample volume captured in the cylinder.

4.3.3. Solid Phase Subsampling (D3) after the first Dilbit Pool Fire (Test 3.1)

The first 2-m dilbit pool fire, Test 3.1, was run on February 6, 2019. Post-burn solids samples were collected the next morning on February 7. The total weight of solids recovered from the pan was 69.25 lb (31.48 kg).

The solids took two general forms:

- (i) Thin, brittle, porous grey and black crust, analogous to a raised pie crust with air underneath, effectively covering the entire pan.
- (ii) A thick, glass-like, low-porosity solid that settled into low areas underneath the crust. This material did not have air underneath and had to be chipped out of the pan with a chisel.

Three spot samples of solid residue were collected from the pan. One was taken from pan center, a second from half radius, and a third at the full radius (outer perimeter). Photos of the residue in the pan on February 7 are shown in Figure 4-6 and Figure 4-7 just prior to collecting the grab samples for offsite analysis.



Figure 4-6. Photo of post-burn solids remaining after Test 3.1. Total mass of solids was measured at 31.48 kg.



Figure 4-7. Close-up photo of sampling post-burn residue from the center of the pan for Test 3.1 on February 7.

4.3.4. Solid Phase Subsampling (D5) after the last Dilbit Pool Fire (Test 3.6)

Post-burn solids samples for test 3.6 were collected on March 5, one day after completion of the last 2-m dilbit pool fire. A photo of the pan contents is shown in Figure 4-8. The residue was qualitatively similar to that described for residue left after the first dilbit pool fire in section 4.3.3. Spot samples were collected as described in section 4.3.3 and total mass of solids in the pan was measured. The spot samples were packaged and shipped offsite for analysis.



Figure 4-8. Photo of post-burn solids remaining after test 3.6. Total mass remaining was measured at 19.60 kg.

4.4. Dilbit Crude Analysis Methods

4.4.1. Analysis of Sampling Events D1, D2, D4

Dilbit samples were analyzed for selected physical properties as well as pressurized and unpressurized composition. A summary of physical properties tested on samples obtained in unpressurized “Boston Round” bottles is given in the list below.

- Initial Boiling Point by ASTM D8003 (ASTM 2015)+ ASTM D7169 (ASTM 2016a) Merge
- Flash Point, Closed Cup by ASTM D3828 (ASTM 2016h)
- Water and Sediment by ASTM D4007 (ASTM 2016f)
- Water content by Karl Fischer
- Density @15°C by ASTM D5002M (ASTM 2013a)
- Heat of Combustion by ASTM D240 (ASTM 2014)
- Sulfur by ASTM D4294 (ASTM 2016e)
- Viscosity by ASTM D445 (ASTM 2018)

- Hydrogen Sulfide and Mercaptans by UOP 163 (UOP 2010)

A summary of physical properties tested on samples obtained in pressurized floating piston cylinders (FPC) compliant with GPA 2174-14 pressurized sampling includes:

- VPCR_x(T) by ASTM D6377-M (ASTM 2016b) at selected temperature and expansion points listed in Table 3-2
- Pressurized Compositional Analysis by ASTM D8003 (ASTM 2015) + ASTM D7169 (ASTM 2016a) + GOR merge

The ASTM D6377-M VPCR methodology used for the dilbit samples was the same as for the Bakken samples described in section 3.4.2.1. Whole oil composition listed above was obtained by combining ASTM D8003-15 measurements, ASTM D7169 measurements, and GOR flash measurements by numerical recombination. Doing so yielded whole oil descriptions with components to include N₂+O₂, CO₂, carbon number groups including major isomers from C1-C24, and a lumped heavy portion given as C25+.

5. EXPERIMENTAL RESULTS

This chapter presents the analytical results for the heptane, Bakken crude, and dilbit collected and analyzed as described in Chapters 2-4. Recall these analyses were conducted in support of a series of pool fire tests run on the same fuels at the Sandia Thermal Test complex. Description and results of the pool fire testing are given in a separate report by Luketa, Cruz-Cabrera et al. (2019).

5.1. General statement on fuels comparison

A summary of basic physical properties of the three fuels tested here is given in Table 5-1. Properties such as mass density, sulfur content, VPCR, and heat of combustion provide a basic profile relevant to identification, handling, and testing. Heptane represents a refined product with a combination of density, viscosity and VPCR that facilitate easy handling at ambient conditions. Bakken represents a light, sweet crude oil with a wide boiling range and sufficient light ends content and VPCR that pressurized storage and specialized handling were imposed to retain stable properties throughout months of storage time required to complete the test series described here and elsewhere (Luketa, Blanchat et al. 2019). The dilbit, a heavy sour crude, was the most dense and viscous fluid tested here. Even so, the dilbit also contained sufficient light ends content that pressurized storage and specialized handling were imposed, similar to the Bakken. Recall from section 4.3.1 that a specialized recirculation system using a pneumatic diaphragm pump was required to overcome the viscosity and adequately mix the dilbit for sampling. Gross heats of combustion on a mass basis were similar across all three fuels.

Table 5-1. Summary of average fuel properties observed in this study

Property	Units	<i>n</i> -Heptane	Bakken	Dilbit
Density (15.56°C)	kg/m ³	687.5	805.9	923.9
API Gravity (60°F)	°	74.1	43.9	21.7
Sulfur	mass%	0.00	0.1	3.6
VPCR _{0.2} (37.8°C)	kPa	10.9 ^a	136	93
Viscosity (40°C)	mm ² /s	0.005 ^b	2.0	71.9
Heat of Combustion	MJ/kg	47.8	46.8	43.0

^a Vapor pressure for *n*-heptane calculated using process simulator. Verified using correlation from literature (Williamham, Taylor et al. 1945).

^b Viscosity for *n*-heptane calculated using correlation from literature (Sagdeev, Fomina et al. 2013). Verified via process simulator.

5.1.1. Fuel Visual Properties

Example photos of heptane (12/6/17), Bakken crude (1/31/2018) and diluted bitumen (2/27/2019) in clear glass bottles subsampled during this study are shown side-by-side in Figure 5-1. The heptane was clear, the Bakken exhibited a muddy dark green color, and the diluted bitumen was dark black. Generally speaking, crude oil color is driven by the heavy component contents, so the darker the color, the heavier the oil. Though not captured specifically in these photos, the Bakken also produced a mustard-colored foam several inches deep that formed on top of the liquid phase as it was drawn from pressurized storage into the unpressurized bottle. The foam broke up after a few minutes and settled to the stable configuration that is shown in the photo.



Figure 5-1. Comparison of heptane (left), Bakken (center) and diluted bitumen (right) visual properties captured during bottle sampling.

5.2. *n*-Heptane Analysis Results

Results received from the analysis laboratory are given in Figure 5-2. The *n*-heptane purity measured at 99.5 vol% compares well with the analysis certificate that accompanied the delivery from the supplier (see Appendix C). Other measured values such as average molecular weight, density at ambient pressure/temperature conditions, and heat of combustion compare well with reference database values obtained from the U.S. Department of Commerce National Institute of Standards and Technology (NIST). By verifying the supplier purity and comparing these properties with those of *n*-heptane from a standards database, it is reasonable to say that these samples were representative of a high-purity *n*-heptane.

Table 5-2. Analysis results for composite heptane sample collected from the 9 heptane drums delivered to Sandia.

Test	Measured Value	Unit	Method	NIST Reference Value	Unit	Comment
Chemical Formula	C ₇ H ₁₆		N/A			
Heptane Purity	99.5	Vol %	ASTM D6730			
Average Molecular Weight	102.14	g/mol	Frz Pt Depression	100.2	g/mol	
API Gravity @ 60°F	74.1	°API	ASTM D4052			
Density @ 15.56°C	0.6875	g/cm ³	ASTM D4052	0.6876	g/cm ³	T = 15.6C, P = 1 atm
Relative Density, 15.56°C/15.56°C	0.6882		ASTM D4052			
Gross Heat of Combustion	20558	BTU/lb	ASTM D240	20710	BTU/lb	
Water Content	25	mg/kg	ASTM E1064			
Corrected Flash Point	<50	°F	ASTM D93			
Flash/No Flash	Flash	°F	ASTM D3828			
Target Flash Point	-5	°F	ASTM D3828			

5.3. Crude Oil Unpressurized Properties

5.3.1. Bakken Physical Properties (Sampling Event B1 – Loading Site)

Measured physical properties for the Bakken sample taken at the loading site in North Dakota (B1) are listed in Table 5-3. The oil is considered a light, sweet crude according to the API gravity (42.9°) and total sulfur content (0.0844 wt%)(API 2011).

Table 5-3. Physical properties of Bakken samples taken at loading site (B1).

Method	Test	Result	Unit
ASTM D5002	API Gravity @ 60°F	42.9	°API
ASTM D5002	Relative Density @ 60/60°F	0.8107	
ASTM D4294	Sulfur Content	0.0844	Wt %
ASTM D445	Kinematic Viscosity 40 °C	1.996	cSt
ASTM D93A	Corrected Flash Point	<50	°F
ASTM D664A	Acid Number	< 0.10	mg KOH/g
ASTM D3230	Salt Content (as electrometric chloride)	3.8	lb/1000bbl
UOP 163	H2S	< 1	ppm Wt
UOP 163	Mercaptan Sulfur	<3	ppm Wt
ASTM D1159	Average Bromine Number	1.1	
ASTM D97	Pour Point	<-33	°C
ASTM D97	Pour Point	<-27.4	°F
ASTM D4007	Sediment And Water	<0.05	Vol %
ASTM D4928	Sample Temp - Before Mixing	24	°C
ASTM D4928	Sample Temp - After Mixing	24	°C
ASTM D4928	Water Content	0.01	Vol %
ASTM D6560	Asphaltene Content	< 0.50	Wt %
ASTM D5762	Nitrogen Content	430	ppm Wt
UOP 269	Basic Nitrogen	130.0	ppm Wt
ASTM D4530	Average Micro Method Carbon Residue	0.53	Wt %
ASTM D240	Gross Heat of Combustion	20,834	BTU/lb
ASTM D482	Average Ash	0.003	Wt %
ASTM D5708A_MOD	Iron	1.30	mg/kg
ASTM D5708A_MOD	Nickel	<0.100	mg/kg
ASTM D5708A_MOD	Sodium	7.30	mg/kg
ASTM D5708A_MOD	Vanadium	<0.100	mg/kg
UOP 46	Wax Content	< 5.0	Wt %
UOP 375	UOP Characterization Factor (K)	12.11	
ASTM D7359	Total Fluorine	<1.00	mg/kg
ASTM D7359	Total Chlorine	1.20	mg/kg
ASTM D4929B	Organic Chloride in Orig. Sample-Crude Oil	< 1.0	µg/g
ASTM D5291	Carbon Content	75.00	Wt %
ASTM D5291	Hydrogen Content	10.00	Wt %
ASTM D5291	Nitrogen Content	0.10	Wt %

5.4. Fuel Compositions

5.4.1. *Bakken Whole Oil Composition*

Pressurized composition from fluid samples taken at five sampling events (Events B1, B2, B4, B6, and B8) are shown graphically in Figure 5-2 and Figure 5-3. Additional compositional data for each event are shown with black outlined bars of the same color. For replicates, two-cylinder samples were taken back-to-back from the same source and analyzed. The legends for these charts organize the samples by sampling event (Event B1, B2, B4, B6, or B8) and the replicate number for that event (B1-1 or B1-2, for example). The reader should note there is an analytical process difference for the dissolved gas compositions determined under the DOE/DOT/TC-sponsored work (Events B1, B2, B8) versus the NRC/TC work (Events B4, B6). The underlying analytical method (GPA 2103-M(GPA 2003)) used in the DOE/DOT/TC work did not differentiate between O₂ and N₂, thus their contributions to the whole oil were lumped (N₂ + O₂) and are represented only as N₂ in Figure 5-2. The method used in the NRC/TC work, ASTM D8003 merge method, did differentiate and the separate components are shown in Figure 5-2.

For the dissolved gas compositions shown in Figure 5-2, there appeared to be a spike in N₂ in the first replicates of the B1, B6, and B8 samples, though the second replicates do not show the same feature. There are several possible explanations for this behavior. First, it is possible that sample handling during acquisition in the field, during the required transfer from the manual piston cylinders (MPC) to the 1-L piston cylinders (for the B6 subsamples), or during cylinder hookup to the analytical instruments in the lab introduced air into the system. Another possibility is that air could have also been introduced into the tanker during storage times (weeks to months) under periodic vacuum conditions at lower temperatures when the vapor pressure of the oil was less than the ambient pressure. The fact that paired samples (i.e., B1-1 and B1-2, or B6-1 and B6-2) pulled from the same tanker load just minutes apart showed variability similar or greater in magnitude than observed between samples separated by months suggests that the inherent sample-to-sample variability is a more likely explanation than air ingestion into the tanker.

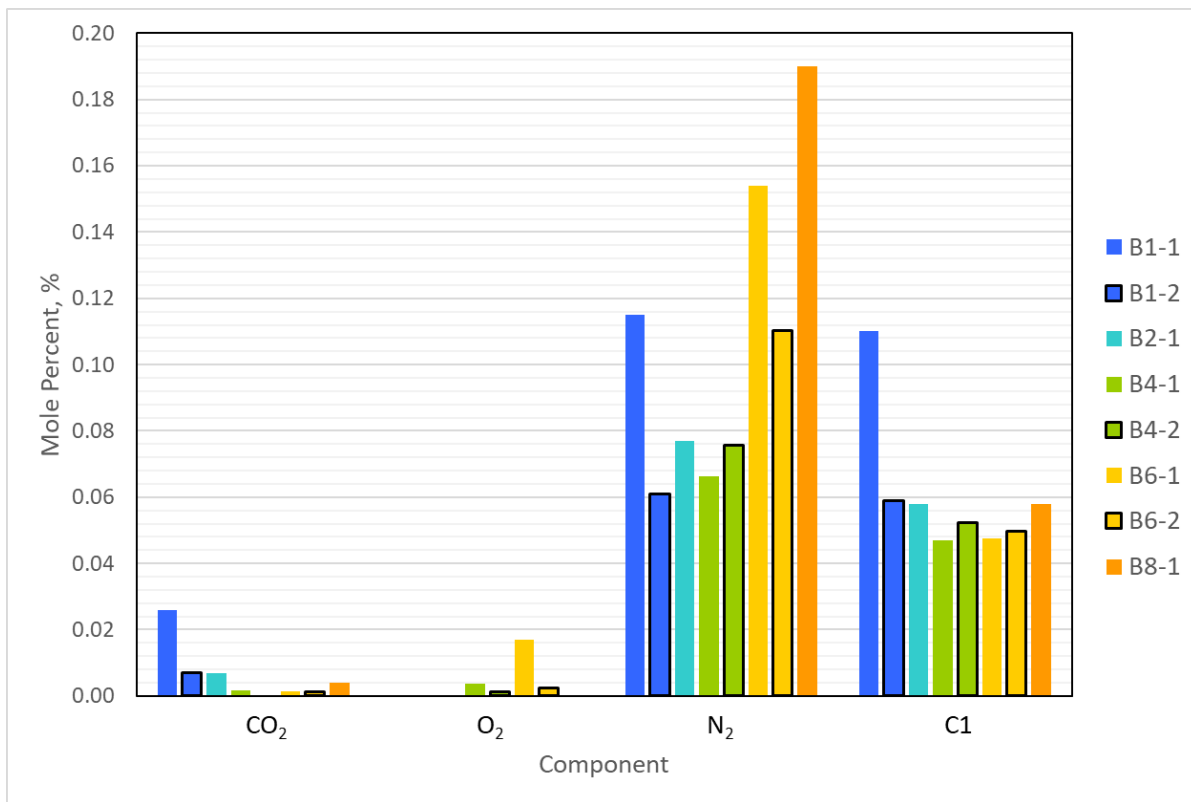


Figure 5-2. Dissolved gas compositions (N₂, C1, CO₂) in Bakken samples taken at loading and at the Sandia burn site.

The light hydrocarbons in Figure 5-3 showed little variation across all subsamples. The light end compositions held nearly constant across all the subsamples, providing evidence that the custom Sandia pressurized tanker and sampling methods did not allow escape of these components from the main sample of oil in the tanker and provided consistent fuel properties for the 2-m pool fire test series.

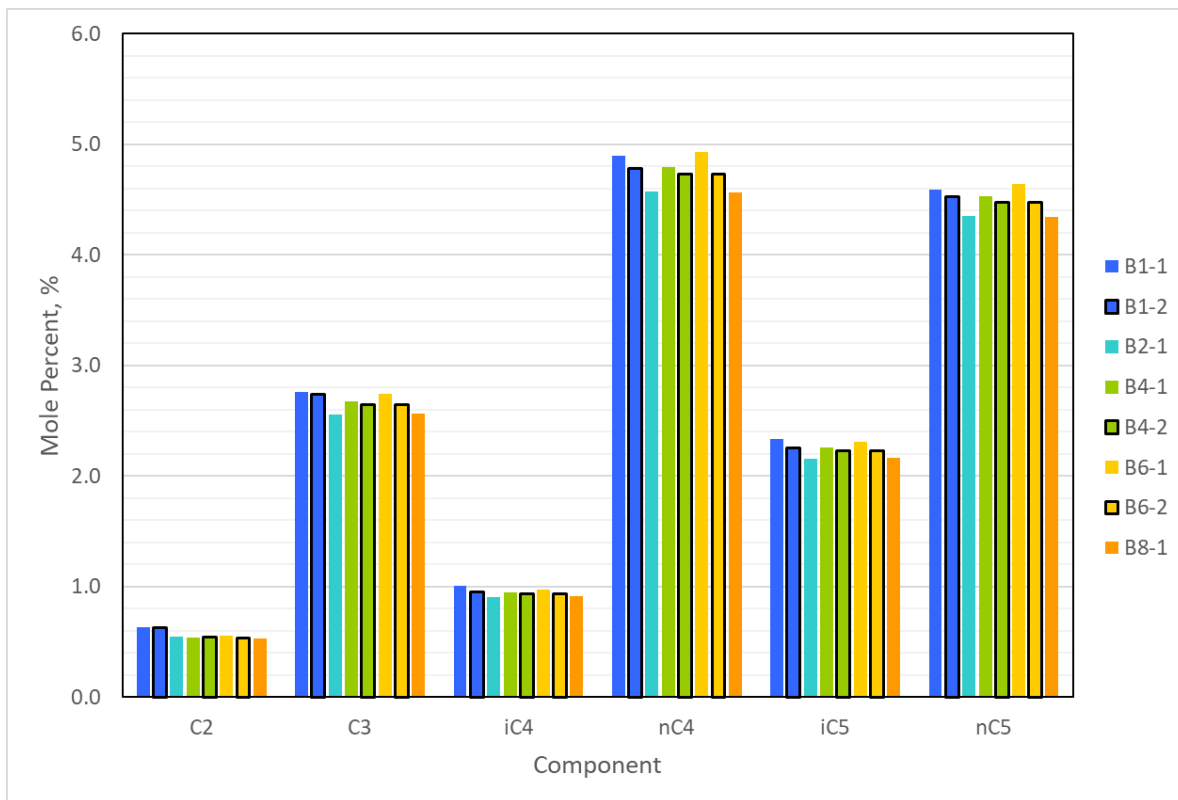


Figure 5-3. Light ends compositions (C2-nC5) in Bakken samples taken at loading and at the Sandia burn site.

Whole oil carbon number plots for the samples are given graphically as line plots in Figure 5-4, with tables of the data in Appendix C. Note dissolved gases (N₂, CO₂, etc.) are included in the whole oil composition (see Figure 5-2) but are not visible at the scale shown. The compositional analyses for events B1, B2, and B8 were determined by numerical merge on a suite of analytical measurements by GPA 2103-M + ASTM D2887 + ASTM D7169. Alternatively, B4 and B6 were determined by a merge of ASTM D8003 + GOR + ASTM D7169 measurements. The different compositional methods were used because these phases of the research project (B1,2,8 versus B4,6) were funded by different sponsors, and were brought together here under a sharing agreement. Details of these methods are described in a separate report (Lord, Allen et al. 2018). A close look at Figure 5-4 indicates that the four whole oil curves with higher C7-C8 peaks around 13-15 mole% were associated with the GPA 2103-M merge method (referred to in Figure 5-4 as TM1), while the four whole oil curves with lower C7-C8 peaks around 10-12 mole% were associated with the ASTM D8003 merge method (referred to in Figure 5-4 as TM2). The differences in C7-C8 are likely associated with how the middle hydrocarbons measured in the analytical procedures were binned into carbon number groups during the analytical data reduction and merge processes. As described in Lord, Allen et al. (2018), both the GPA 2103-M and ASTM D8003 merge methods were found to return whole oil compositions that were generally comparable to those from a baseline flash separator method for representative Bakken and Eagle Ford crude samples captured and analyzed in 2016-2017. While it appears there is a slight method bias, the authors do not have a basis for determining which set of whole oil curves determined via TM1 or TM2 is more accurate in this application.

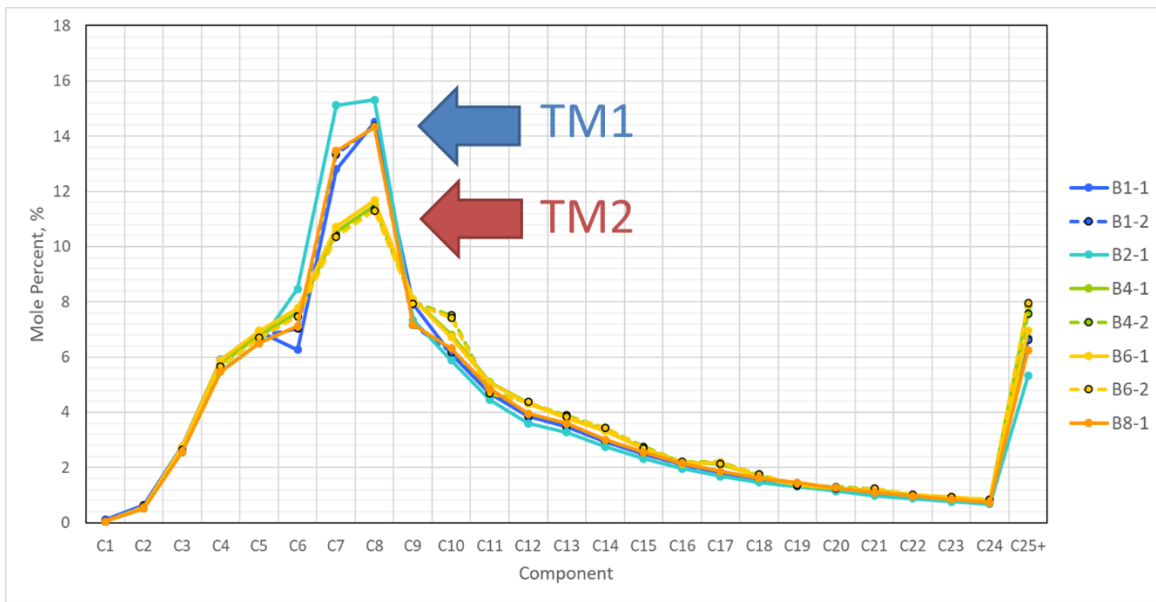


Figure 5-4. Whole oil carbon number plots for Bakken oil sampled at loading and burn sites listed by sampling event and replicate number.

5.4.2. Dilbit Whole Oil Composition

Pressurized compositions from fluid samples taken at three sampling events are shown graphically in Figure 5-5 and Figure 5-6. One replicate was taken for each of these sampling events. The legends for these charts organize the samples by sampling event and replicate, similar to what was done for the Bakken subsamples in the previous section.

The dissolved gas compositions are shown in Figure 5-5. Despite N₂ presence in the oil because of the tank loading methodology (see section 4.1), the N₂ contents seen here are the same scale as the Bakken N₂ content. At first glance, there appeared to be a spike in N₂ in the D2 sample. Similar to what was described in section 5.4.1 for the Bakken compositions, inherent sample-to-sample variability is a more likely explanation than any of the other effects.

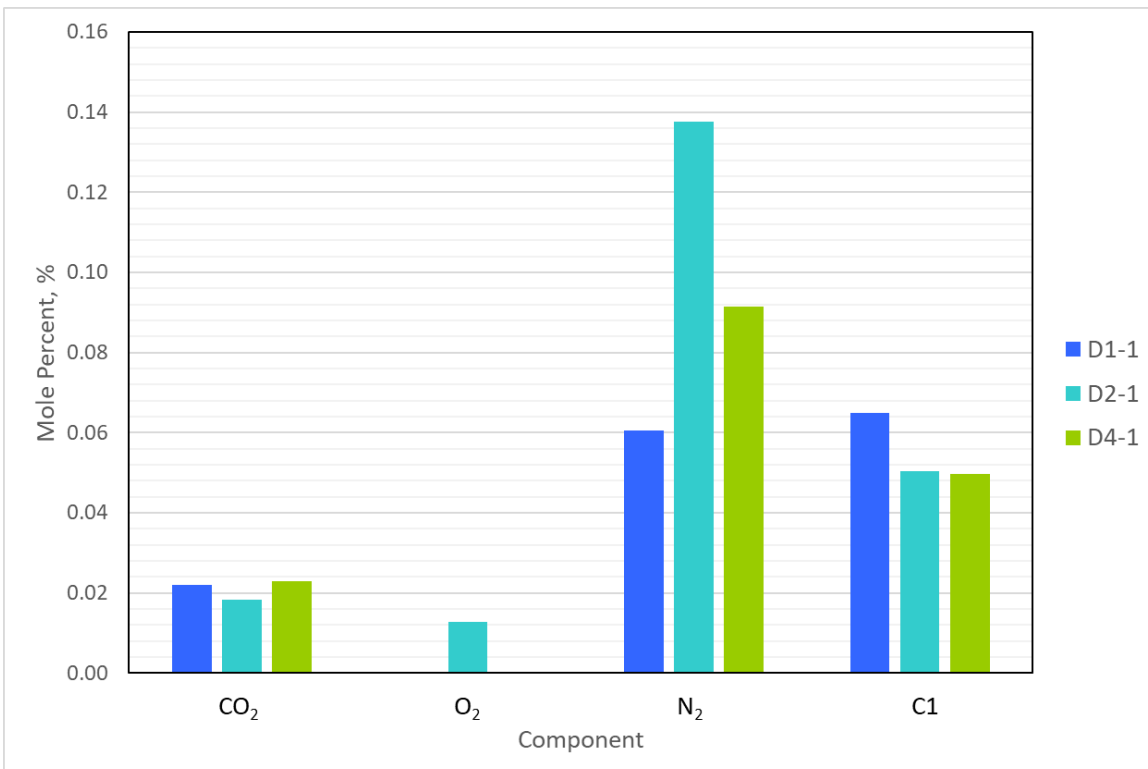


Figure 5-5 Dissolved gas contents for the dilbit subsamples at initial subsampling in December and at Sandia's thermal test complex.

The hydrocarbons in Figure 5-6 showed little variation across all subsamples. The light end compositions held nearly constant across all the subsamples, providing evidence that the propane storage tanks and subsequent sampling methods did not allow escape of these components from the oils in the tanks and provided consistent fuel properties for the 2-m pool fire test series.

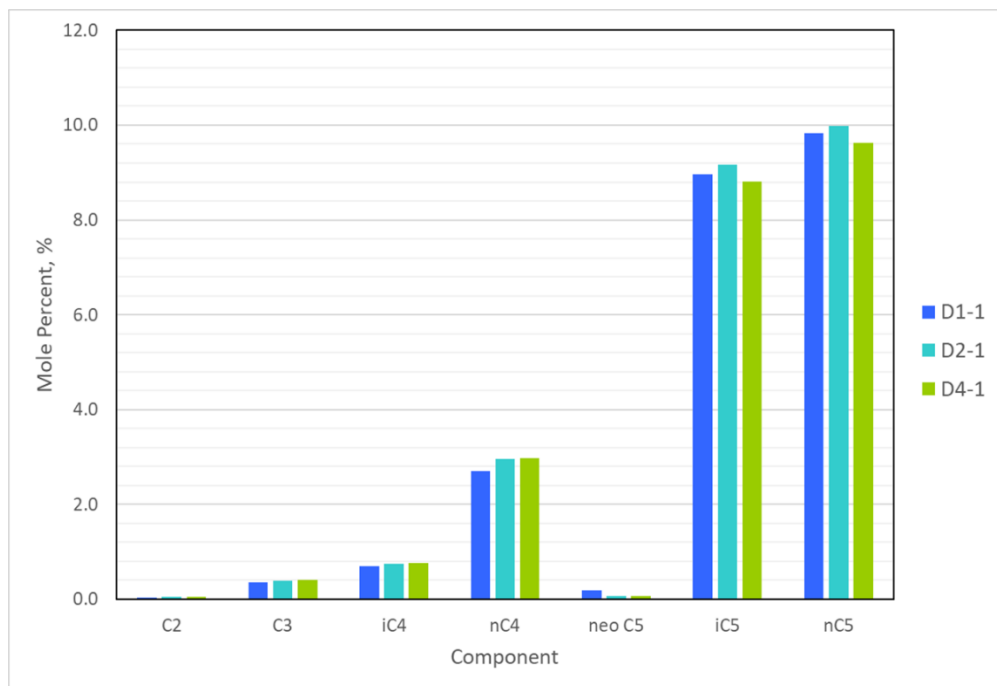


Figure 5-6 Light ends (C2-nC5) measured for the dilbit subsamples

Whole oil carbon number plots for the samples are given graphically in Figure 5-7, with tables of the data in Appendix C. In general, the whole oil compositions changed little across the three subsamples. Of note, there was a large spike at C5, a shallow local minimum around C11, and a large C25+ residual content across all three samples. This distribution is expected for diluted bitumen, which comprises a mixture of bitumen, a heavy sour oil, and a diluent, which is a condensate or mixture of light hydrocarbons, blended so that the resulting fluid meets pipeline specifications for viscosity and density. Bitumen alone would be problematic to transport via pipeline due to its inherently high viscosity. The amount and type of diluent added to the base bitumen material depends upon the price and availability of diluent and specifications for transport of the combined material. The diluent in this case is associated with the peak in mole% around C5, and the base bitumen material is associated with the heavier materials from about C10 up. While normal for dilbit, this carbon number distribution is distinct from other crudes tested in this research study that exhibit a peak in the C7 to C8 range along with a rapidly descending “tail” above C10 (recall Figure 5-4 above or see Luketa, Blanchat et al. (2019)). Additional discussion of the diluent and base bitumen compositions that comprise the dilbit samples is presented in section 6.2.

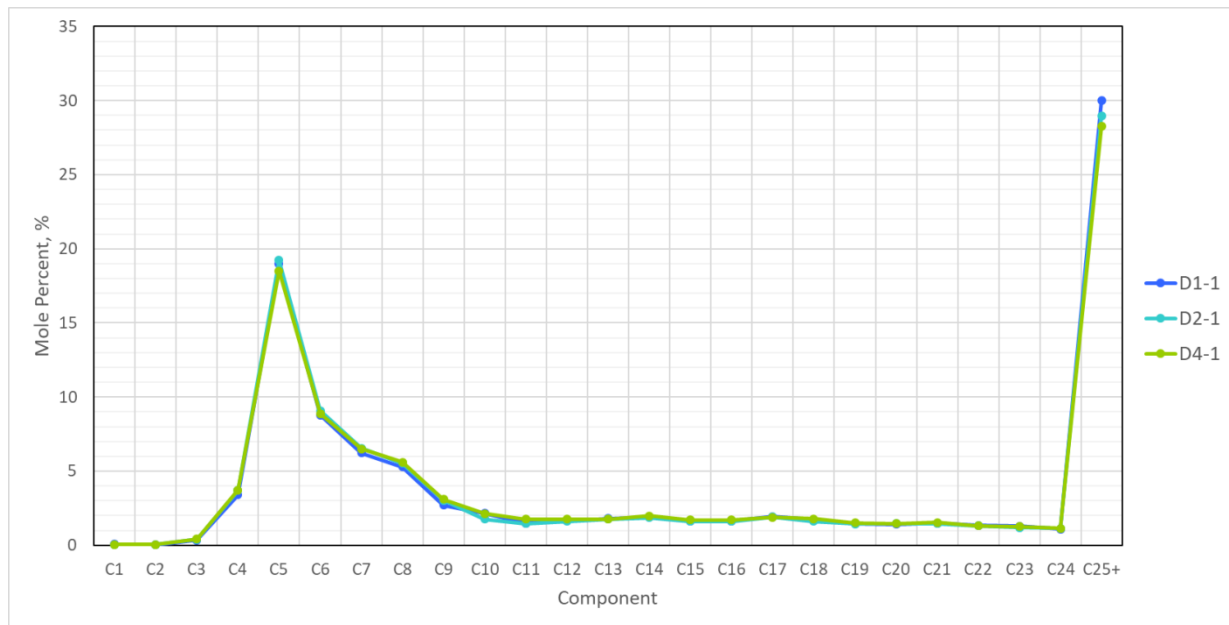


Figure 5-7 Whole oil compositions measured for the dilbit subsamples

5.5. Fuel Vapor Pressures

5.5.1. Bakken $VPCR_x(37.8^\circ C; 100^\circ F)$ Results

$VPCR_x(37.8^\circ C; 100^\circ F)$ results for the Bakken loading and burn site samples are summarized in Figure 5-8. Duplicate samples were collected and measured for all of the sampling events, so the error bars in the figure represent 2 times the standard deviation among those replicates. Pressure units are given in kPa on the left axis and psia on the right axis.

Of particular interest for this study are the $VPCR_x$ for events B4 and B6, which represent the properties just prior to the first and last pool fires in the series run in January 2018. Events B1, B2, and B8 provide some context for what was measured from tanker samples obtained in August 2017, October 2017, and July 2018, respectively.

Starting at the right end of the chart with $V/L = 4$, $VPCR_4(37.8^\circ C; 100^\circ F)$ was nominally 75 kPa (11 psia) for samples from events B4 and B6. Moving to lower V/L , the vapor pressure $VPCR_x$ increases to 135-150 kPa (20-22 psia) for events B4 and B6 at $V/L = 0.2$. $VPCR_x$ data were not gathered at $V/L = 1$ and $V/L = 2$ for events B1, B2, and B8 because they were outside the scope of work under US DOE/DOE/TC.

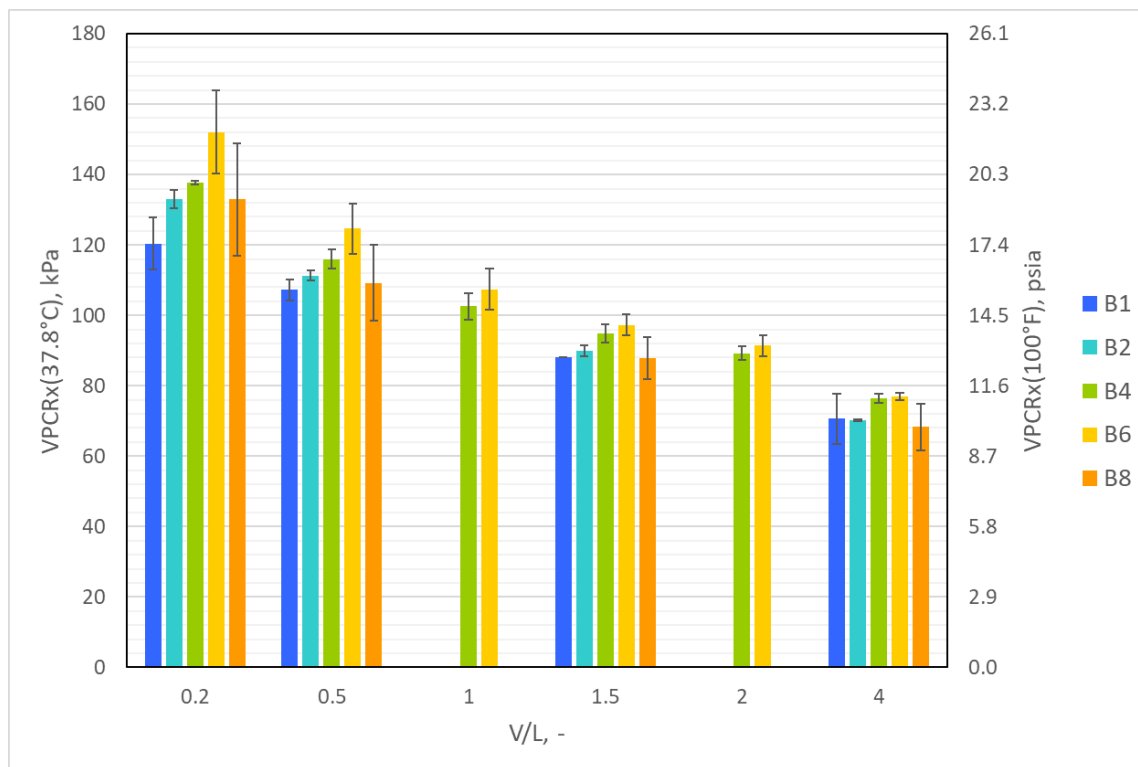


Figure 5-8. Pressure-expansion column charts showing measured $VPCR_x(100^{\circ}\text{F}; 37.8^{\circ}\text{C})$ for the Bakken loading samples (B1) and burn site samples (B2, B4, B6, and B8).

A prior Sandia study (Lord, Allen et al. 2017) indicated that the $VPCR_{0.2}(37.8^{\circ}\text{C}; 100^{\circ}\text{F})$ point is a reasonable indicator of bubble point pressure at that temperature, which can be a useful reference property. For the oils tested here, the average $VPCR_{0.2}(37.8^{\circ}\text{C}; 100^{\circ}\text{F})$ for each sampling event is given in Table 5-4. These data indicate that the bubble point pressures of the Bakken oil at $T = 100^{\circ}\text{F}; 37.8^{\circ}\text{C}$ appear to range from 120-152 kPa (17.5-22.0 psia) depending on the sampling event.

Table 5-4. Average measured $VPCR_{0.2}(37.8^{\circ}\text{C}; 100^{\circ}\text{F})$ for the five Bakken sampling events.

Event	Description	$VPCR_{0.2}(37.8^{\circ}\text{C}; 100^{\circ}\text{F})$
B1	Loading	120 kPa (17.5 psia)
B2	Burn 1	133 kPa (19.3 psia)
B4	Burn 2	138 kPa (20.0 psia)
B6	Burn 3	152 kPa (22.0 psia)
B8	July 2018	133 kPa (19.3 psia)

All of the VPCR points collected on the Bakken oil in this work, including $V/L < 0.2$, are reported in Appendix B.

5.5.2. Bakken $VPCR_x(50^{\circ}\text{C}; 122^{\circ}\text{F})$ Results

$VPCR_x$ at 50°C or 122°F are reported as they are relevant to Transport of Dangerous Goods (TDG) regulations. $VPCR_x(50^{\circ}\text{C}; 122^{\circ}\text{F})$ results for the Bakken burn site samples are summarized in Figure 5-9. Only one sample at this temperature was measured for sampling events B4 and B6. Pressure units are given in kPa on the left axis and psia on the right axis.

Starting at the right end of the chart with $V/L = 4$, $VPCR_4(50^\circ\text{C}; 122^\circ\text{F})$ was nominally 97 kPa (14 psia) for samples from events B4 and B6. Moving to lower V/L , the vapor pressure $VPCR_x$ increases to 165-175 kPa (24-25 psia) for events B4 and B6 at $V/L = 0.2$.

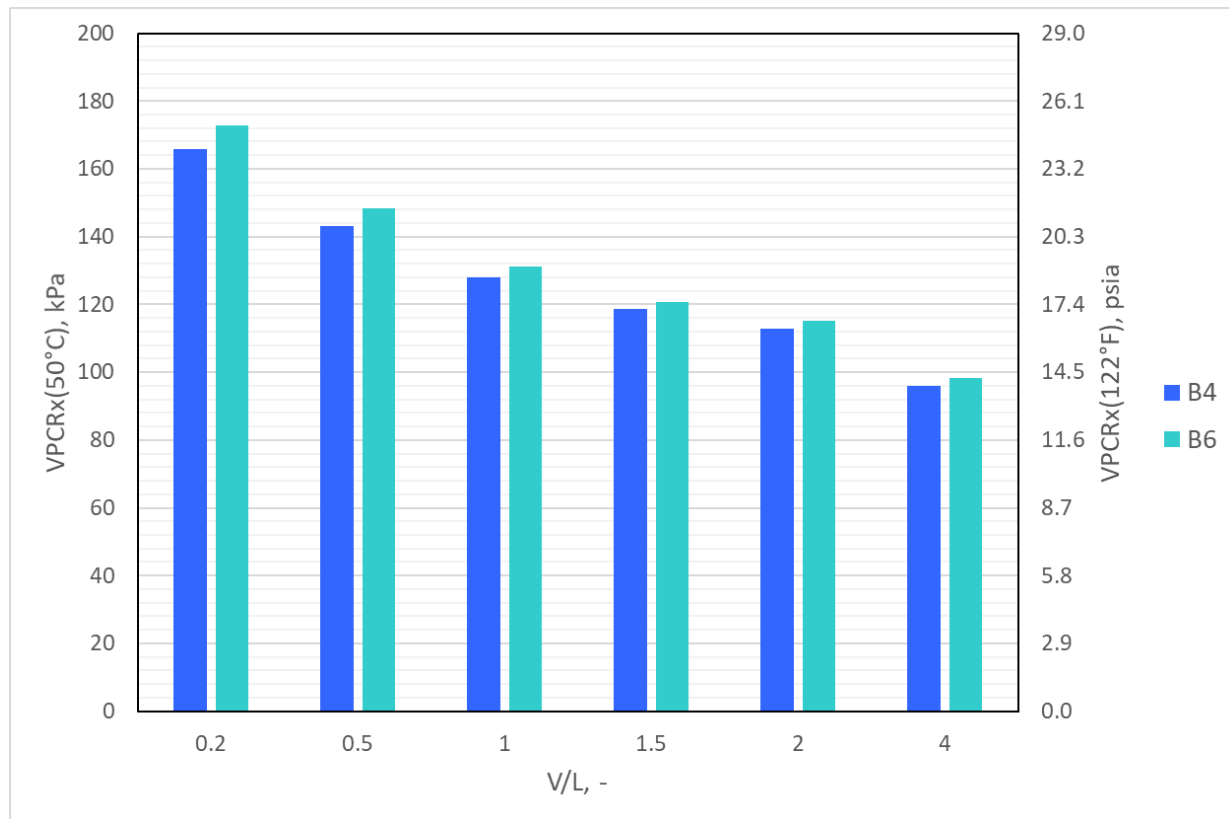


Figure 5-9. Pressure-expansion column charts showing measured $VPCR_x(50^\circ\text{C}; 122^\circ\text{F})$ for the Bakken burn site samples (B4 and B6).

5.5.3. Dilbit $VPCR_x(37.8^\circ\text{C}; 100^\circ\text{F})$ Results

$VPCR_x(37.8^\circ\text{C}; 100^\circ\text{F})$ results for the dilbit loading and burn site samples are summarized in Figure 5-10. Pressure units are given in kPa on the left axis and psia on the right axis. Of particular interest for this study are the $VPCR_x$ for D2 and D4, which represent the properties just prior to the first and last pool fires in the series run in Luketa, Blanchat et al. (2019). Starting at the right end of the chart with $V/L = 4$, $VPCR_4(37.8^\circ\text{C}; 100^\circ\text{F})$ was nominally 55 kPa (8 psia) all three samples. Moving to lower V/L , the vapor pressure $VPCR_x$ increases to 85-98 kPa (12-14 psia) at $V/L = 0.2$.

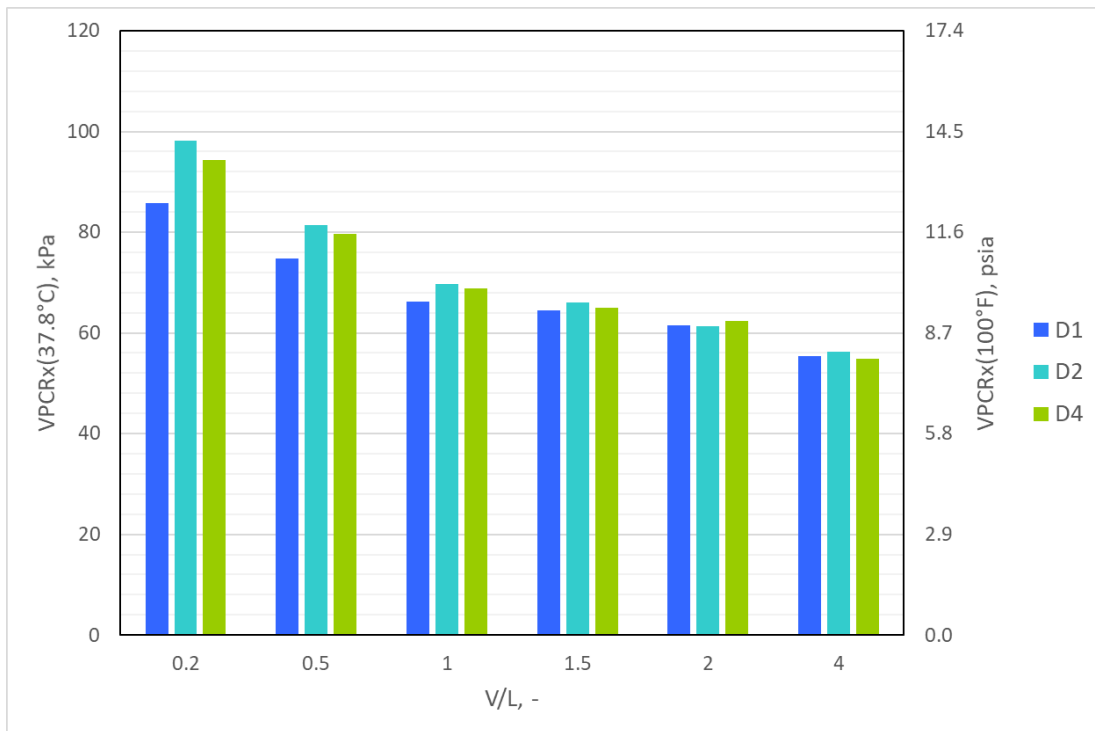


Figure 5-10. Pressure-expansion column charts showing measured $VPCR_x(37.8^\circ\text{C}; 100^\circ\text{F})$ for the dilbit baseline samples (D1) and burn site samples (D2 and D4).

As stated previously, $VPCR_{0.2}(37.8^\circ\text{C}; 100^\circ\text{F})$ is a reasonable indicator of bubble point pressure at 37.8°C (100°F). For the oils tested here, the average $VPCR_{0.2}(37.8^\circ\text{C}; 100^\circ\text{F})$ for each sampling event is given in Table 5-5. These data indicate that the bubble point pressures of the dilbit at $T=37.8^\circ\text{C}$; 100°F appear to range from 85.7-98.1 kPa (12.4-14.2 psia).

Table 5-5. Average measured $VPCR_{0.2}(37.8^\circ\text{C}; 100^\circ\text{F})$ for the three dilbit sampling events.

Event	Description	$VPCR_{0.2}(100^\circ\text{F}; 37.8^\circ\text{C})$
D1	Loading	85.7 kPa (12.4 psia)
D2	Burn Site 1	98.1 kPa (14.2 psia)
D4	Burn Site 2	94.4 kPa (13.7 psia)

5.5.4. Dilbit $VPCR_x(122^\circ\text{F}; 50^\circ\text{C})$ Results

$VPCR_x(122^\circ\text{F}; 50^\circ\text{C})$ results for the dilbit burn site samples are summarized in Figure 5-11. Starting at the right end of the chart with $V/L = 4$, $VPCR_4(122^\circ\text{F}; 50^\circ\text{C})$ was nominally 80 kPa (11.5 psia) for the three samples. Moving to lower V/L , the vapor pressure $VPCR_x$ increases to 115-135 kPa (17-20 psia) at $V/L = 0.2$.

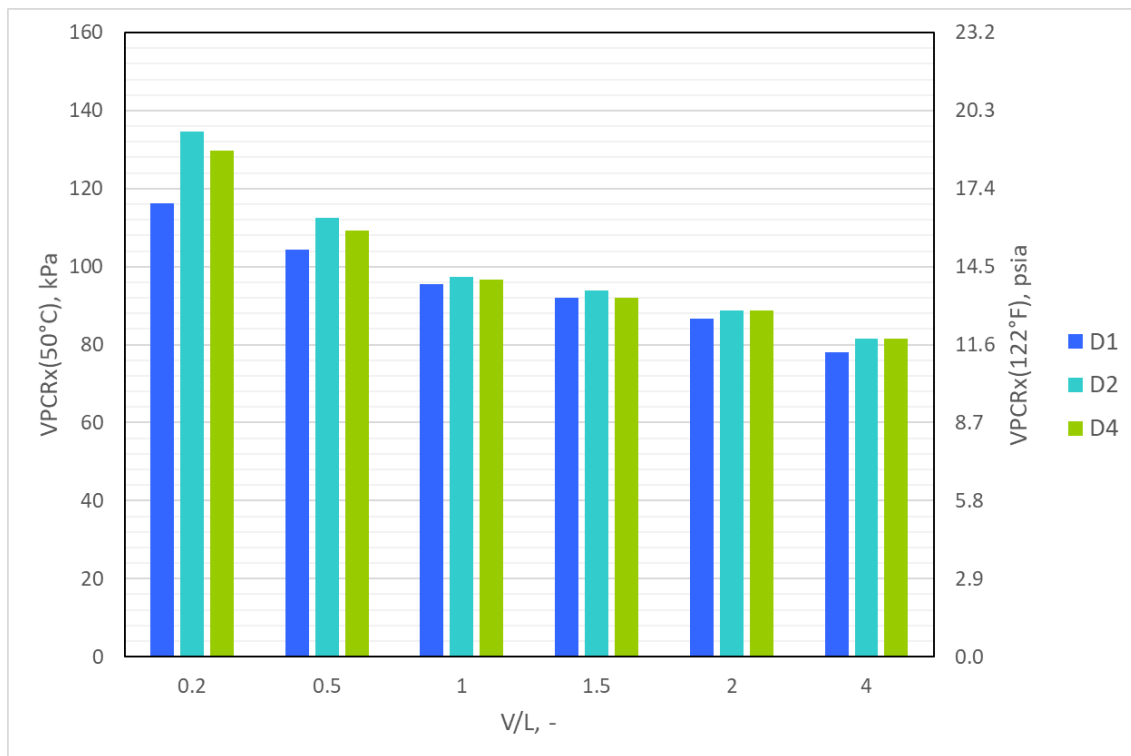


Figure 5-11. Pressure-expansion column charts showing measured $VPCR_x(50^\circ\text{C}; 122^\circ\text{F})$ for the dilbit samples.

5.5.5. *Equation of State-Modeled $VPCR_x(T)$*

The compositional data were used as received from the analytical laboratories and passed through an equation of state (EOS) model to simulate $VPCR_x$ at 37.8°C (100°F) and 50°C (122°F). These results are shown in Figure 5-12Error! Reference source not found. through Figure 5-15Error! Reference source not found.. The average of measured $VPCR_x$ replicates (given by solid bars) for each sampling event are given with EOS-modeled $VPCR_x$ from $V/L = 0.2$ to 4 (shown as striped bars). Error bars shown for the EOS-modeled $VPCR_x$ represent twice the standard deviation between simulations using different measured compositions from the same sampling event. Since only one composition was measured for each of the B2 and B8 sampling events, no error bars are shown. The magnitude of deviation between the measured $VPCR_x$ values and the EOS modeled $VPCR_x$ values are consistent with sample to sample variations observed between cylinders in prior work by the authors (Lord, Allen et al. 2017).

Bakken results are given in Figure 5-12Error! Reference source not found. and Figure 5-13Error! Reference source not found.. In particular, the first compositional replicates for Bakken subsamples B1 and B6 showed high N_2 levels (see Figure 5-2). These correlated to larger EOS-modeled $VPCR_x(100^\circ\text{F}; 37.8^\circ\text{C})$ in Figure 5-12Error! Reference source not found., especially at low V/L .

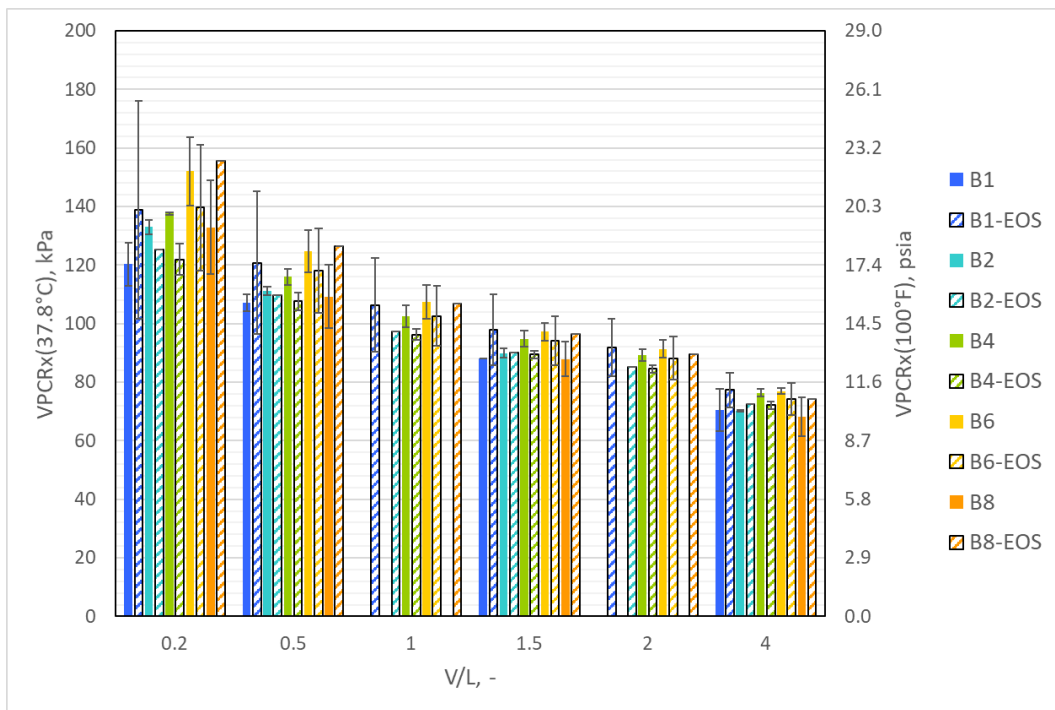


Figure 5-12. Column chart comparing measured $VPCR_x$ to EOS-modeled $VPCR_x$ for Bakken loading and burn site samples at $T = 100^{\circ}\text{F}$; 37.8°C . Measured values are solid bars with 2σ error bars, modeled values are striped bars.

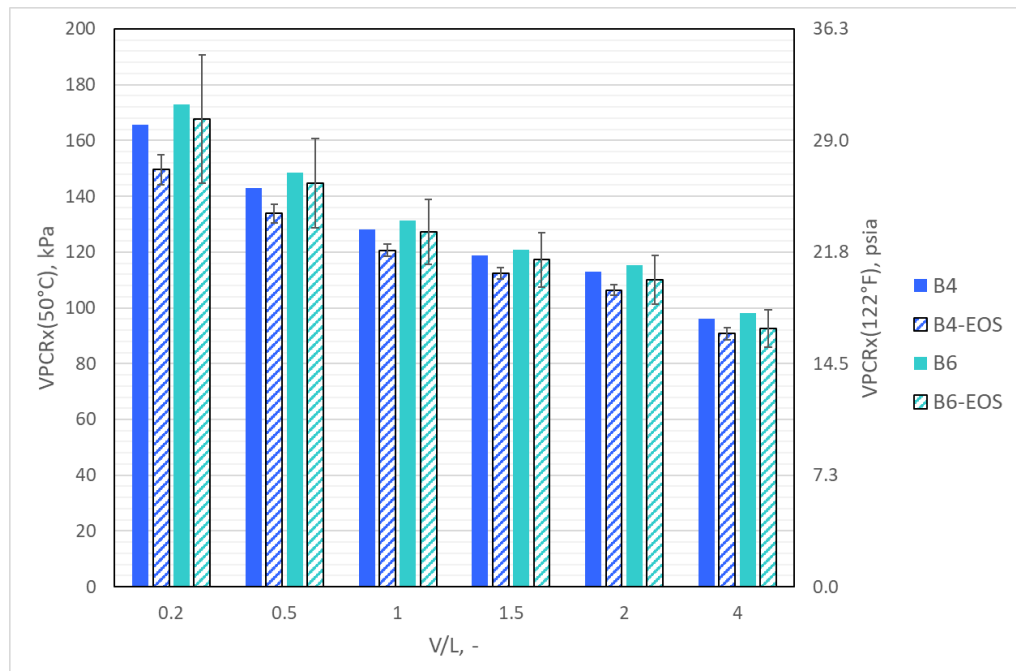


Figure 5-13 Column chart comparing measured $VPCR_x$ to EOS-modeled $VPCR_x$ for Bakken burn site samples at $T = 50^{\circ}\text{C}$; 122°F . Measured values are solid bars, modeled values are striped bars.

Dilbit VPCR_x results are given in Figure 5-14**Error! Reference source not found.** and Figure 5-15**Error! Reference source not found.**. No error bars are shown for the measured or EOS-modeled VPCR_x since no additional replicates were analyzed in either case. The reasonable agreement between measured and modeled VPCR_x indicates that the compositions and vapor pressures measured for these oils are self-consistent, and that the EOS model performance for VPCR_x in this pressure and temperature range is reasonably accurate. A close review of the higher temperature 50°C case reveals a bias, however: the EOS-modeled VPCR_x values are all around 10-15% lower than the measured values. This same bias is not seen in the T = 37.8°C case. The authors pose several possible explanations for this temperature sensitivity in EOS performance. A primary factor is likely associated with the diluent composition, dominated by C5 and C6 components, many of which exhibit pure component boiling points in the range from 37.8 to 50°C. The EOS-simulated heating appears to volatilize less material, indicated by lower simulated VPCR_x, than the actual heating. There is a practical necessity to lump the continuum of different components that actually appear in a crude into bins, in this case by carbon number, for facilitating laboratory reporting and subsequent modeling. It is possible that this simplification was more compatible with EOS performance and VPCR calculations at T = 37.8°C than at 50°C. Another possibility is that some of the EOS empirical tuning parameters, namely binary interaction coefficients (BICs), that were likely optimized by the EOS software vendor for a wide range of oils, were not optimized for dilbit. The dilbit is an extreme case of co-existence of large concentrations of light and heavy end carbon molecules that may require some attention to tuning BICs for those component pairs.

The general finding from the EOS modeling effort is that the measured VPCR_x for each sample correlates well with the underlying composition, providing confidence that the property measurements and compositional measurements are sufficiently accurate and self-consistent for the purpose of this work.

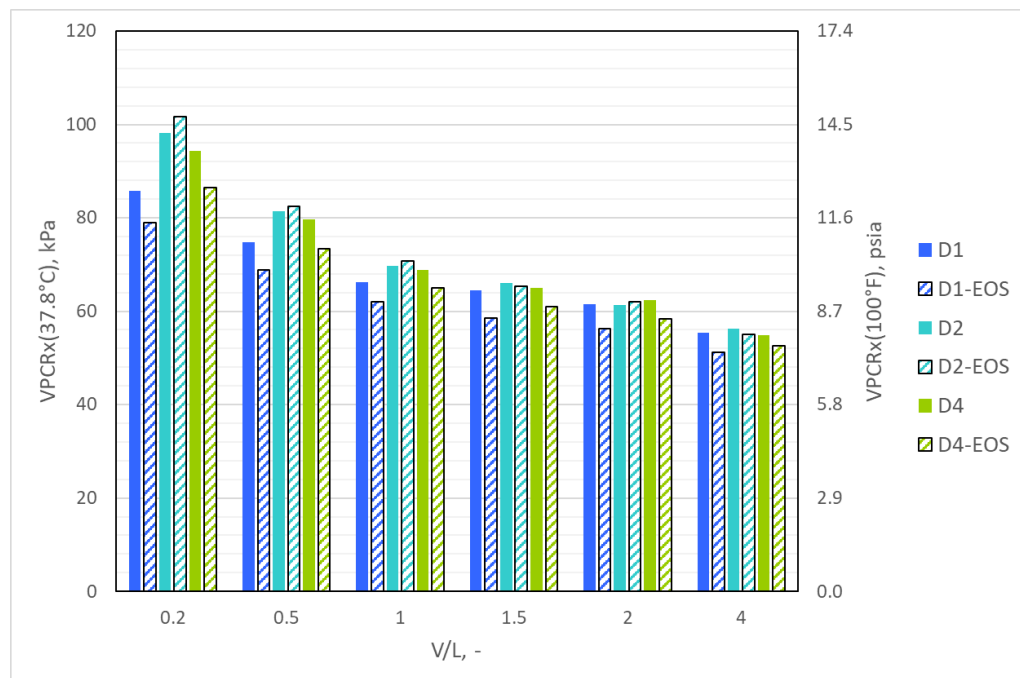


Figure 5-14. Column chart comparing measured VPCR_x to EOS-modeled VPCR_x for dilbit loading and burn site samples at T = 37.8°C; 100°F. Measured values are solid bars, modeled values are striped bars.

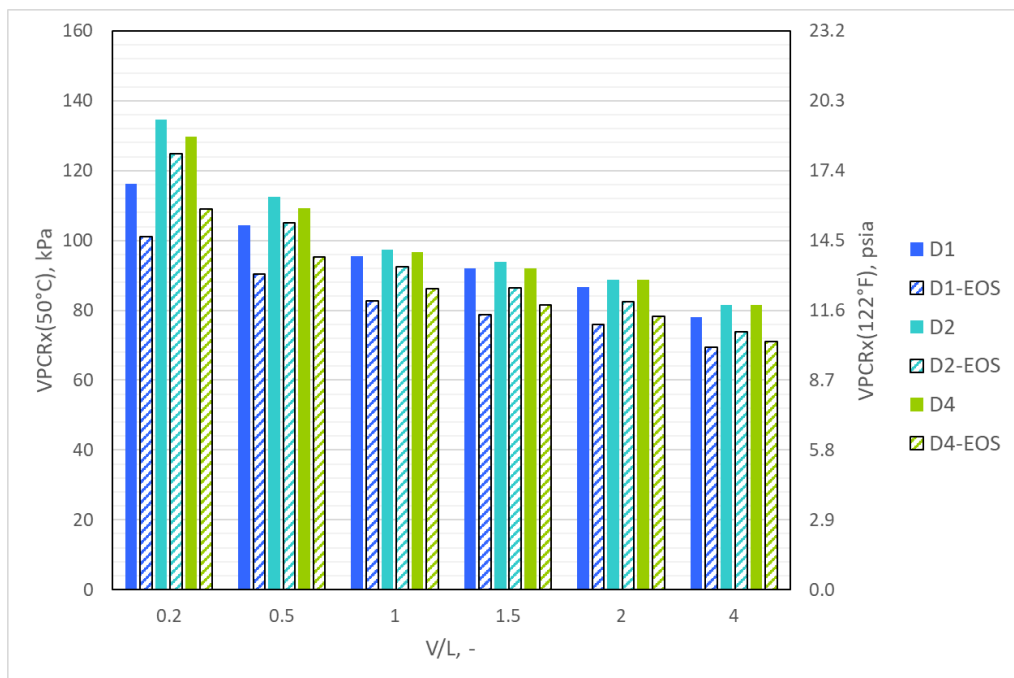


Figure 5-15 Column chart comparing measured VPCR_x to EOS-modeled VPCR_x for dilbit samples at T = 50°C; 122°F;. Measured values are solid bars, modeled values are striped bars.

5.6. Other Selected Properties

5.6.1. Other Bakken Properties

Physical properties from fluid samples taken for the Bakken crude at the four different sampling events are shown in Table 5-6. The $\text{VPCR}_{0.2}(37.8^\circ\text{C}; 100^\circ\text{F})$ data are reproduced from section 5.5.1. Heat of combustion for samples B4 and B6 are around 46.0 MJ/kg, which is typical of a hydrocarbon liquid fuel (Luketa, Blanchat et al. 2019). Note that subsamples B1, B2, and B8 underwent different methods for determining density, water content and flash point than events B4 and B6, as listed in the table below. The density was measured with a digital density analyzer (ASTM D5002), within 0.3% through time. For water content, ASTM D4377 referenced potentiometric Karl Fischer titration (range: 0.02-2 % water), while ASTM D6304 was for coulometric Karl Fischer titration (range: 0.001-2.500 % water). The water contents were low for subsamples B1, B2, B4, and B8. The water content for subsample B6 was an order of magnitude larger than the others and hints at the possibility of small amounts of entrained water, as explained in Section F.3.2.5 of the corresponding DOE/DOT/TC project report (Luketa, Blanchat et al. 2019). ASTM D93A, D56A, and D3828 all used closed cup testers to determine flash points, though ASTM D93A and D56A required a slow, constant heating rate, and ASTM D3828 specified isothermal testing at discrete temperatures. Measured flash points were at the lower limits of resolution ($< 10^\circ\text{C}$; $< 50^\circ\text{F}$ and $< -30^\circ\text{C}$; $< -22^\circ\text{F}$) for the methods used. ASTM D3828 covers tests within a range of -30°C to 300°C , while the ASTM D56A test results only applied down to 10°C ; 50°F . The Bakken crude flashed at the lower temperature limit of the laboratory setup (1°C ; 34°F) using ASTM D93A and D56A, but the test methods indicated that the analyst should begin checking when the sample is 10°C (18°F) below the expected flash point, so $< 10^\circ\text{C}$ ($< 50^\circ\text{F}$) was reported, though the actual observed flash point was $\leq 1^\circ\text{C}$ ($\leq 34^\circ\text{F}$). The viscosity for subsample B1 was similar to that measured for other light oils, which is higher than condensate streams, but smaller than many blends commonly seen in pipelines (Enbridge Pipelines and Enbridge Energy Partners 2018). The initial boiling points were measured for B4 and B6 using ASTMD8003 + ASTM D7169 merge.

Table 5-6. Physical properties of Bakken samples taken at loading site and Sandia burn site.

Property	Unit	Method	B1	B2	B4	B6	B8
Description			Loading	Burn Site 1	Burn Site 2	Burn Site 3	July 2018
Sampling Date			8/17/2017	10/2/2017	1/18/2018	1/31/2018	7/18/2018
VPCR_{0.2} (37.8°C; 100°F)	kPa	ASTM D6377-M	120	133	138	152	133
Density (15.6°C; 60°F)	kg/m ³	ASTM D5002-M	812.3	811.3	809.6	810.0	812.4
Sulfur	wt%	ASTM D4294	0.0844	--	--	--	--
Heat of Comb.	MJ/kg	ASTM D240	48.5	49.3	46.0	46.0	44.1
Water Content	wt%	ASTM D4377	0.012	0.016	--	--	0.009
Water Content	wt%	ASTM D6304	--	--	0.01	0.16	--
Flash Point	°C; °F	ASTM D93A	< 10; < 50	--	--	--	--
Flash Point	°C; °F	ASTM D56A	--	< 10; < 50	--	--	< 10; < 50
Flash Point	°C; °F	ASTM D3828	--	--	< -30; < -22	< -30; < -22	--
Viscosity (40°C; 104°F)	mm ² /s	ASTM D445	1.996	--	--	--	--
Initial Boiling Point	°C; °F	ASTM D8003 + D7169 merge	--	--	-42.2; -44.0	-42.2; -44.0	--

5.6.2. Other Dilbit Properties

Physical properties from fluid samples taken for the dilbit at three different sampling events are shown in Table 5-7. Subsample D1 was taken from tank 5, subsample D2 from tank 12, and subsample D4 from tank 9. This is different from the Bakken subsamples, which were taken from the same tanker at several points through time. Thus, the dilbit data shown in the table do not represent a change in properties of one material through time, but rather, a glimpse into the properties of three separate samples from three different tanks on three different dates. Most of the properties listed showed little variation among the tanks, which is expected because the tanks were filled from the same pipeline source over the course of two days. The VPCR_{0.2}(37.8°C; 100°F) data were reproduced from section 5.5.3, and show a 1.8 psia variation, which is typical at V/L = 0.2. Heats of combustion for the samples were around 43.0 MJ/kg, which is typical of a hydrocarbon liquid fuel. The water contents for the dilbit were high relative to approximations of the water solubility, which were calculated from density and elemental hydrogen content to be somewhere around 0.1 wt% (Amani, Gray et al. 2014). Water is ever-present in the production and processing of dilbit, so it is actively removed to help meet the pipeline specification of < 0.5 wt% basic sediment and water. The water contents measured here are consistent with the pipeline specifications, yet may indicate free-phase water in the samples. The dilbit flashed at the lowest temperature for the ASTM D3828 setup, thus they are listed as < -30°C; < -22°F. There was about 10% variation in the measured viscosity, which is high relative to variation that would have been expected had the same sample been measured, as shown in the test method (ASTM 2018). Additionally, these viscosities measured high relative to historical records of comparable dilbits, which list viscosity at 40°C between 50-55 mm²/s (Enbridge Pipelines and Enbridge Energy Partners 2012; Enbridge Pipelines and Enbridge Energy Partners 2018). The initial boiling points were measured using ASTM D8003 + ASTM D7169 merge.

Table 5-7. Physical properties of dilbit samples taken at loading site and Sandia burn site.

Property	Unit	Method	D1	D2	D4
Description			Loading	Burn Site 1	Burn Site 2
Sampling Date			12/3/2018	1/28/2019	2/27/2019
Sample Tank			5	12	9
VPCR_{0.2} (37.8°C; 100°F)	kPa	ASTM D6377-M	85.7	98.1	94.4
Density (15°C; 59°F)	kg/m ³	ASTM D5002-M	923.5	924.2	923.9
Sulfur	wt%	ASTM D4294	3.68	3.65	3.42
Hydrogen Sulfide	ppm	UOP 163	6	0	2
Mercaptans	ppm	UOP 163	114	100	120
Heat of Comb.	MJ/kg	ASTM D240	42.8	43.1	43.2
Water Content	wt%	ASTM D4007	0.450	0.200	0.275
Flash Point	°C; °F	ASTM D3828	< -30; < -22	< -30; < -22	< -30; < -22
Viscosity (40°C; 104°F)	mm ² /s	ASTM D445	76.41	70.26	68.99
Initial Boiling Point	°C; °F	ASTM D8003 + ASTM D7169 merge	-0.6; 30.9	-0.6; 30.9	-0.6; 30.9

6. ADDITIONAL OBSERVATIONS

6.1. Comparison of Bakken and Dilbit Properties

Table 6-1 gives a concise comparison of the two crudes tested as part of this project. Oil properties averaged over all sampling events are listed, with the higher of the two in bold. The Bakken crude showed higher vapor pressure than the dilbit, though the dilbit had a higher < C6 content than the Bakken. This may seem counterintuitive at first glance, but further analysis reveals that the dilbit contained > 5.5 wt% C5, while the Bakken crude was around 3 wt% C5. This means that the majority of the material in the dilbit below C6 had relatively low volatility, leading to a lower vapor pressure than the Bakken, which had greater C1-C4 contents. The heats of combustion for the Bakken samples were slightly higher than the heats of combustions for the dilbit samples, though they were both relatively close and within the region expected for hydrocarbons. Since the flash points for both materials were below the lower limit of the test methods, several methods were employed to predict the flash points of each material. These predictions were based on VPCR₄, the temperature at which 10 vol% of the material vaporizes, and the normal boiling point (Alqaheem and Riazi 2017). Each method predicted the Bakken crude to have a lower flash point than the dilbit, though both were calculated to be below the lowest temperature for ASTM D3828 (-30°C; -22°F). The dilbit was approximately 35 times more viscous than the Bakken crude at 40°C, which is expected since the dilbit is a mixture of an extremely viscous base bitumen material that is diluted with light condensate hydrocarbons to meet pipeline specifications.

Table 6-1. A brief comparison of Bakken crude and dilbit properties; bold values represent the larger of the two.

Property	Units	Bakken	Dilbit
VPCR _{0.2} (37.8°C; 100°F)	kPa	136	92.7
Density (15°C; 60°F)	kg/m ³	805.9	923.9
Sulfur Content	wt%	0.08	3.58
< C6 Content	wt%	6.0	6.7
Heat of Comb.	MJ/kg	46.8	43.0
Water Content	wt%	0.06	0.3
Flash Point	°C; °F	< -30; < -22	< -30; < -22
Viscosity (40°C)	mm ² /s	2.0	71.9
Initial Boiling Point	°C; °F	-42.2; -44.0	-0.6; 30.9

6.2. Diluent Composition in the Dilbit

Observations from the pool fire testing described in Luketa, Cruz-Cabrera et al. (2019) indicated that the dilbit exhibited distinct behavior from the Bakken crude in several key combustion parameters, calling for a closer look at the compositional makeup of the dilbit to possibly understand why this occurred.

One important question pertaining to the burns was the compositional breakdown of the diluent, the bitumen, and the diluent-to-bitumen ratio in the dilbit. The carbon number plot in Figure 6-1 shows the average dilbit composition across the loading and burn samples. Also included in the plot are distributions of a condensate from 12/7/2018 (converted from a vol% distribution found at

<https://crudemonitor.ca/condensates>), and a bitumen (neatbit), from 2018 samples (converted from a boiling point distribution taken as part of the Bitumen Assay Program by the government of Alberta). Neatbit is defined in Birn, Osuna et al. (2014) as “..a nearly pure bitumen product containing about 1-2% diluent.” The dilbit supplier noted that the dilbit was likely blended from these two streams. The condensate shows a clear peak at C5, with gradually decreasing composition as carbon number increases. The bitumen contained very little material up to C8, with gradually increasing compositions at C9 and above.

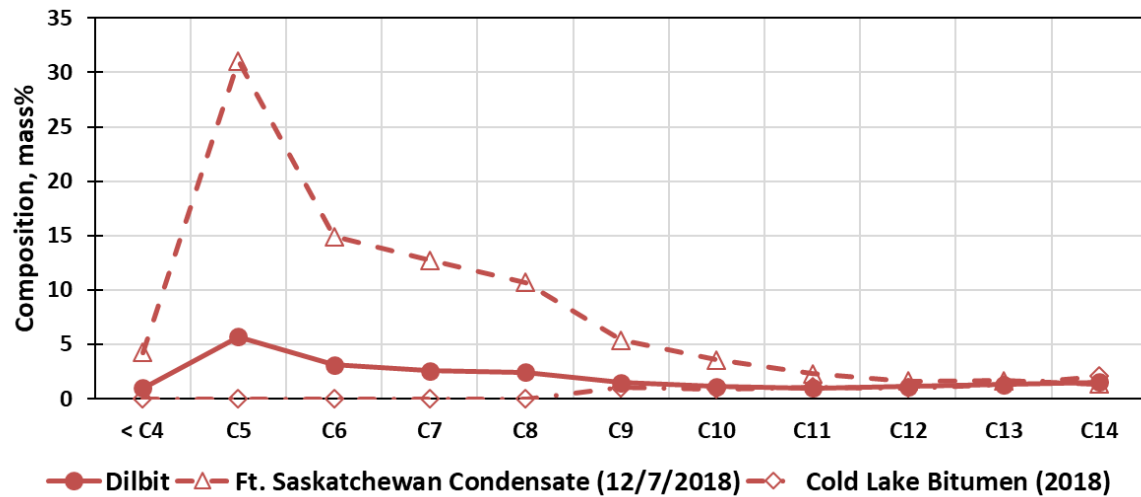


Figure 6-1. C4-C14 compositions for the dilbit fuel alongside a condensate and bitumen that were likely used in the stream.

The condensate and neatbit compositional data were combined using a commercially available process simulator and compared to the loading dilbit sample in Figure 6-2. A mixture of 20-25 vol% condensate and 75-80 vol% bitumen matched the dilbit composition well. According to Sandia contacts in industry, this type of mixture can be found in the supply chain. The composition of such a mixture (22 vol% condensate, 78 vol% bitumen) was plotted below with the dilbit. The calculated mixture showed a local minimum around C12, which is consistent with the minimum observed in the dilbit compositional data. Thus, the diluent in the dilbit caused the spike at C5, while the overlapping diluent and bitumen distributions caused the minimum at C11.

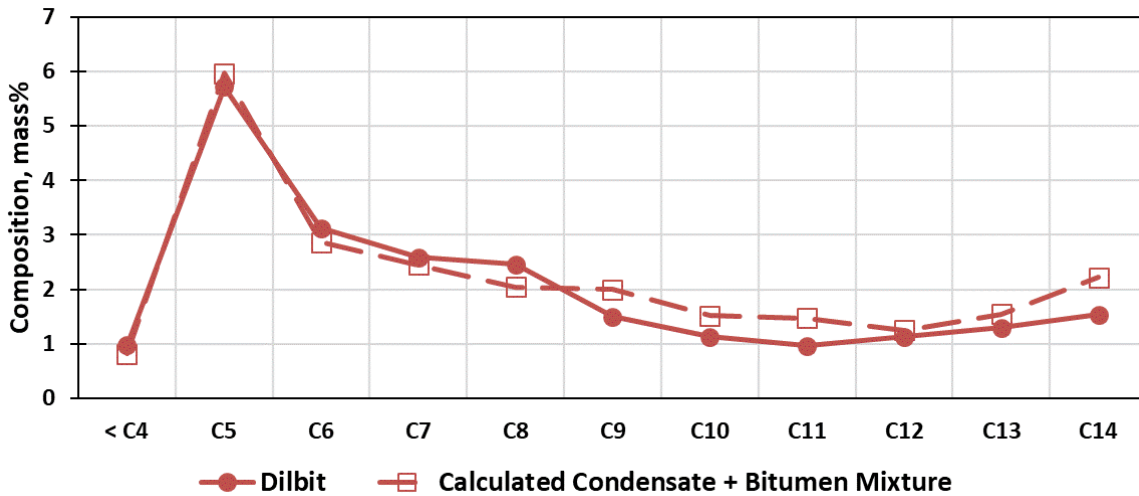


Figure 6-2. Measured C4-C14 composition for dilbit fuel (circle, solid line) and a simulated dilbit composition using likely constituents (square, dashed line).

6.3. Boiling Point Distributions of the Fuels

As mentioned in the parallel Sandia report on burn characteristics (Luketa, Cruz-Cabrera et al. 2019), the dilbit fuel showed transient burn behavior consistent across all the burns that was not seen in the Bakken burns. In Figure 6-3, composition is represented by assigning each component a boiling point and simulating the distillation of the material with increasing temperature using a commercially available process simulator equipped with an Equation of State. Carbon numbers associated with each temperature regime are marked in the plot for reference. Several interesting characteristics can be gleaned from the figure. First, since the *n*-heptane was > 99 mass% pure, nearly all the material would boil off at one temperature. Thus, the *n*-heptane curve is shown as a vertical line near the temperature regime assigned to C7. The Bakken and dilbit oils contained multiple components that would boil at different temperatures, thus resulting in more gradual distributions. Below ~ 95 °C, the Bakken and dilbit boiling point distributions were similar, reaching ~ 12 mass% boiled at 95 °C. Above 95 °C, the Bakken distributions climb smoothly before leveling off around 500 °C – echoing a smoothly decreasing carbon number distribution. The dilbit curves show three basic regimes: steeply increasing mass% with temperature up to 100 °C (slope = 0.13 mass%/°C), a less steep region between 100-250 °C (slope = 0.06 mass%/°C), and steeply increasing mass% with temperature above 250 °C (slope = 0.14 mass%/°C). This behavior indicates a dip in the carbon number distribution between C7 and C12 relative to the overall distribution, which was verified in the previous section.

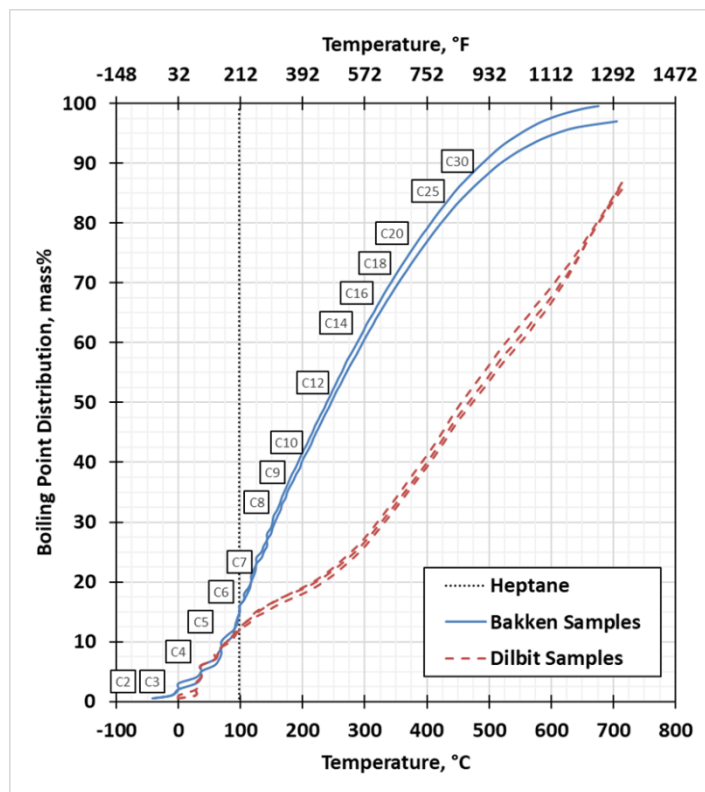


Figure 6-3 Temperature vs. boiling point distribution for the fuels in the burn series

6.4. Density vs. VPCR

Some perspective on where these oil properties fall relative to other oils in the North American supply chain may be gained from reviewing a plot of $VPCR_4(37.8^{\circ}\text{F})$ versus density (60°F), shown in Figure 6-4**Error! Reference source not found.**. A brief summary of the data sources and the measurement methods are given in Table 6-2. In the figure, ASTM D6377-measured $VPCR_x$ values (closed symbols) are shown where available.

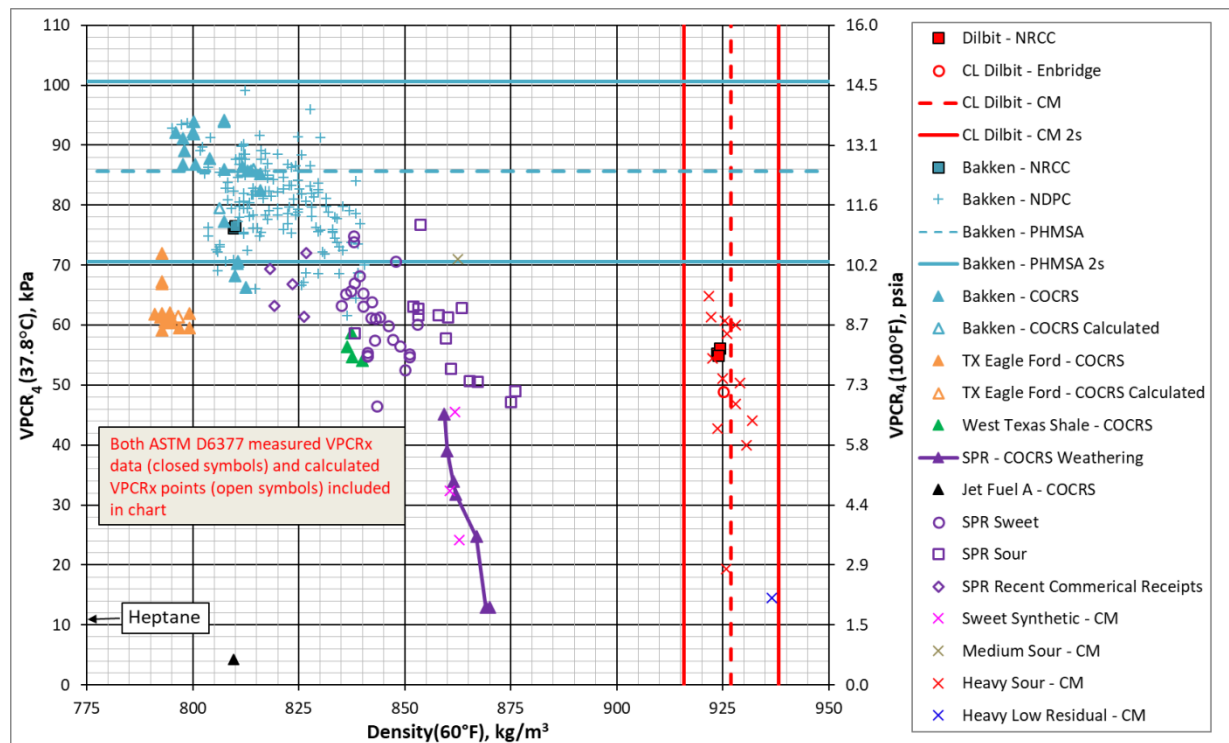


Figure 6-4: Overlay of density vs $VPCR_4(37.8^\circ C)$ for oils from SPR, PHMSA, NDPC and DOE/DOT/TC COCRS with the fuels tested as part of this project.

For systems where only compositional data were available, calculated $VPCR_x$ points (open symbols) are shown based on equation of state calculations. Note that PHMSA did not list individual density values, so the mean $VPCR_4$ and 2 standard deviation (2σ) lines from that body of data were computed and added to the figure. Likewise, CrudeMonitor tracked the density, but not $VPCR_x$, of a representative dilbit (Cold Lake dilbit, abbreviated CL) through time. Thus, the mean density and 2 standard deviation (2σ) lines from that body of data over the past ten years were computed and added to the figure.

As densities increase in the figure, smaller $VPCR_4$ values were observed for incrementally lighter oils, with three notable exceptions: dilbit, the heavy sour streams from CrudeMonitor, and jet fuel. Dilbit was a combination of diluent (very light constituents) and bitumen (very heavy constituents) blended to achieve low enough viscosity to meet pipeline specifications. The diluent comprises light components which drive vapor pressure, while the bitumen comprises heavy ends which drive the density. Thus, the dilbit occupies an interesting place on the plot. The heavy sour streams from CrudeMonitor were stated to exhibit seasonality, which includes strategic blending of light and heavy constituents depending on ambient conditions. This effect is captured by the wide band on the CL dilbit density. Jet fuel was a specific cut of C9-C13 hydrocarbons with no light ends and no heavy ends that is specifically engineered for jet engine performance. Thus, fluids blended or engineered to optimize other properties (flashpoint, viscosity, vapor pressure, etc.) occupy different zones on the density vs. $VPCR_4$ plot than crudes that are only lightly-conditioned.

The fuels from this study occupy interesting spots in the parameter space compared to other historical data. The Bakken-NRC oil exhibited around the same VPCR and density as the NDPC, PHMSA, and COCRS Bakken oils – VPCR₄ ranged from about 70-100 kPa (10-14 psia) with a mean value around 86 kPa (12.5 psia). The dilbit-NRC oil sits close to other dilbit determinations: within the historical density band for CL dilbit from CrudeMonitor, and just 7 kPa (1 psia) above the CL dilbit measurement from Enbridge. The dilbit-NRC oil sits in the middle of a cluster of data from the “Heavy Sour” group on the CrudeMonitor website, which consists of several dilbits. Heptane density ($\rho = 688 \text{ kg/m}^3$) was below the lower limit shown on this chart, though its VPCR₄ was around 12 kPa (1.6 psia).

Table 6-2: Sources and methods for VPCR and Density data in Figure 6-4. Error! Reference source not found.

Plot Label	Source	VPCR _x Method	Density Method
Dilbit – NRC	This Report	ASTM D6377	ASTM D5002
CL Dilbit – Enbridge	(Enbridge Pipelines and Enbridge Energy Partners 2018)	VPCR ₄ at 37.8°C	Not Listed
CL Dilbit – CM	(Crudemonitor 2019)	N/A	Not Listed
Bakken – NRC	This Report	ASTM D6377	ASTM D5002
Bakken – NDPC	(Auers, Couture et al. 2014)	ASTM D6377	ASTM D5002
Bakken – PHMSA	(Auers, Couture et al. 2014; PHMSA 2014)	ASTM D6377	N/A
Bakken - COCRS	(PHMSA 2014; Lord, Allen et al. 2018; Luketa, Blanchat et al. 2019)	ASTM D6377	ASTM D5002
Bakken – COCRS Calculated	(Lord, Allen et al. 2018; Luketa, Blanchat et al. 2019)	Calculated	ASTM D5002
TX Eagle Ford – COCRS	(Lord, Allen et al. 2018; Luketa, Blanchat et al. 2019)	ASTM D6377	ASTM D5002
TX Eagle Ford – COCRS Calculated	(Lord, Allen et al. 2018; Luketa, Blanchat et al. 2019)	Calculated	ASTM D5002
West Texas Shale - COCRS	(Lord, Allen et al. 2018; Luketa, Blanchat et al. 2019)	ASTM D6377	ASTM D5002
SPR – COCRS Weathering	(Luketa, Blanchat et al. 2019)	ASTM D6377	ASTM D5002
Jet Fuel A – COCRS	(Luketa, Blanchat et al. 2019)	ASTM D6377	ASTM D5002
SPR Sweet	SPR Database	Calculated	ASTM D5002
SPR Sour	SPR Database	Calculated	ASTM D5002
SPR Recent Commercial Receipts	SPR Database	Calculated	ASTM D5002

Plot Label	Source	VPCRx Method	Density Method
Sweet Synthetic – CM	(Crudemonitor 2019)	VPCR ₄ at 37.8°C	Not Listed
Medium Sour – CM	(Crudemonitor 2019)	VPCR ₄ at 37.8°C	Not Listed
Heavy Sour – CM	(Crudemonitor 2019)	VPCR ₄ at 37.8°C	Not Listed
Heavy Low Residual – CM	(Crudemonitor 2019)	VPCR ₄ at 37.8°C	Not Listed

Figure 6-5 **Error! Reference source not found.** shows density at 60°F versus VPCR_{0.2}(50°C; 122°F), with a brief summary of the data sources and measurement methods in Table 6-3. The vapor pressure at 50°C is important in regulation of transportation of dangerous goods as a delineation point between a material that is defined as a liquid or a gas (TC 2019). Also, in practical hydrocarbon transportation scenarios, the actual vapor-to-liquid volumes are much less than 4:1 due to economic drivers, with 1% (0.01:1) referenced in ANSI/API (2014). Previous work has shown that uncertainties in ASTM D6377M measurements of VPCR increase as V/L decreases, and V/L = 0.2 was identified as a practical minimum for crude oil with the available technology that correlated well with an independent measure of bubble point pressure (Lord, Allen et al. 2018). Thus, V/L = 0.2 was selected as the smallest V/L for display here. In the plot, there is more variation in the VPCR_{0.2}(50°C; 122°F) values than the VPCR₄(37.8°C; 100°F) data on the previous plot. Data from this study are listed (squares) with those performed in a previous TC study (Prefontaine 2015) and the COCRS (Luketa, Blanchat et al. 2019). The dilbit data from this report fell in the same VPCR_{0.2}(50°C; 122°F) and density region as the dilbits measured in the TC study. The Bakken VPCR_{0.2}(50°C; 122°F) data from this report compared well to the calculated Bakken data from the COCRS. In general, the Bakken VPCR_{0.2}(50°C; 122°F) and density points sat between the light oils and condensates from the TC study.

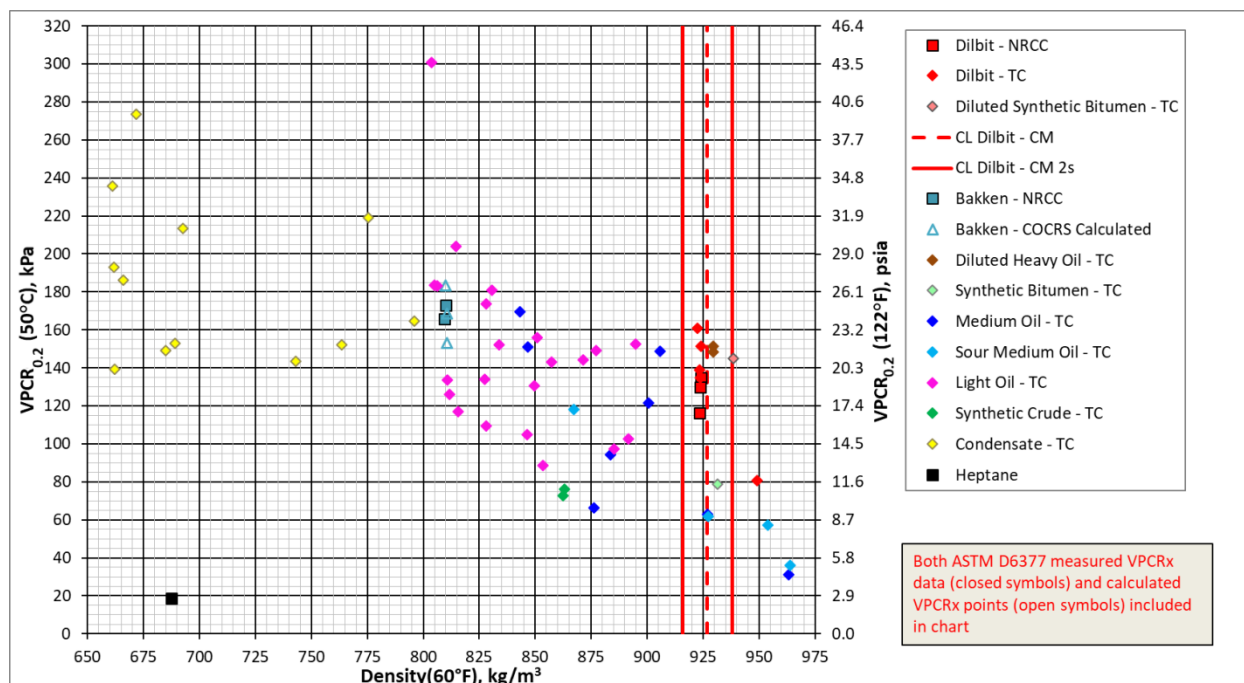


Figure 6-5: Overlay of density vs. VPCR_{0.2}(50°C) for oils from SPR, COCRS, and TC with the fuels tested as part of this project

Table 6-3. Sources and methods for VPCR_x(50°C) and density data in Figure 6-5^{Error! Reference source not found..}

Plot Label	Source	VPCR _x Method	Density Method
Dilbit – NRC	This Report	ASTM D6377	ASTM D5002
Dilbit – TC	(Prefontaine 2015)	ASTM D6377	ASTM D5002
Diluted Synthetic Bitumen – TC	(Prefontaine 2015)	ASTM D6377	ASTM D5002
CL Dilbit – CM	(Crudemonitor 2019)	N/A	Not Listed
Bakken – NRC	This Report	ASTM D6377	ASTM D5002
Bakken – COCRS Calculated	(Luketa, Blanchat et al. 2019)	Calculated	ASTM D5002
Diluted Heavy Oil – TC	(Prefontaine 2015)	ASTM D6377	ASTM D5002
Synthetic Bitumen – TC	(Prefontaine 2015)	ASTM D6377	ASTM D5002
Medium Oil – TC	(Prefontaine 2015)	ASTM D6377	ASTM D5002
Sour Medium Oil – TC	(Prefontaine 2015)	ASTM D6377	ASTM D5002
Light Oil – TC	(Prefontaine 2015)	ASTM D6377	ASTM D5002
Synthetic Crude – TC	(Prefontaine 2015)	ASTM D6377	ASTM D5002
Condensate – TC	(Prefontaine 2015)	ASTM D6377	ASTM D5002
Heptane	Various	Calculated ^a	Supplier Value ^b

^a Vapor pressure for *n*-heptane calculated using process simulator. Verified using correlation from literature (Williamham, Taylor et al. 1945).

^b Density for heptane given in the Certificate of Analysis in Appendix C.

6.5. Post-Burn Solids Mass

6.5.1. Bakken Residue

Post-burn solids from the first and last Bakken pool fires were collected and quantified in Table 6-4. Oil feed (kg) was determined by measuring fuel tank weight before and after each test, and residue (kg) was measured from residue remaining in the pan. The residue ratio (mass residual/mass oil feed) is given for both tests and measured at 0.003 to 0.004. Mean residue ratio for the Bakken pool fire series was 0.003 with standard deviation 0.001.

Table 6-4. Residue mass (kg) and ratio to oil feed (kg/kg) for the 2-m Bakken pool fire series.

Pool Fire Test ID		2.3	2.6
Pool Fire Test Date		1/19/2018	1/31/2018
Sampling Event #		B3	B7
Sampling Description		Post-test residue grab sample + residue mass	Post-test residue grab sample + residue mass
Fuel Supply Temperature	(°C)	20 ± 5	20 ± 5
Fuel Feed Method		Constant Level	Non-continuous fuel feed, allow to burn down
Oil Feed	(kg)	253	203
Residue	(kg)	0.7	0.8
Ratio (Residue/Feed)	(kg/kg)	0.003	0.004

6.5.2. Dilbit residue

Table 6-5 contains a summary of solids remaining after the six tests in the dilbit pool fire series. Tests are listed chronologically. The residue ratio (mass residual/mass oil feed) is given for each test, and ranged from 0.089 to 0.179 depending on test conditions. Mean residue ratio across the six dilbit tests was 0.129, with standard deviation at 0.03. The constant-level fuel feed method with fuel supply temperature at 20 ± 5°C exhibited the most repeatable results for residue ratio, with all four tests in the range 0.117 to 0.139. Allowing the fuel to simply burn down with no fresh feed created the highest residue ratio at 0.179. Test 3.6 where the fuel was heated to 60 ± 5°C left the lowest residue ratio of 0.089. All of the dilbit residue ratios were much higher than observed for the Bakken 2-m pool fire test series summarized in Table 6-4, where ratios measured 0.003-0.004. As such, dilbit left, on average, about 40 times more residue by mass than Bakken in the 2-m pool fire configuration.

Table 6-5. Summary of post-burn solids residue recovered from pan

Pool Fire Test ID		3.1	3.2	3.3	3.4	3.5	3.6
Pool Fire Test Date		2/6/2019	2/14/2019	2/20/2019	2/25/2019	2/27/2019	3/4/2019
Sampling Event		D3	-	-	-	-	D5
Sampling Description		Post-test residue grab sample + residue mass	Residue mass only	Residue mass only	Residue mass only	Residue mass only	Post-test residue grab sample + residue mass
Fuel Supply Temperature	(°C)	20 ± 5	20 ± 5	20 ± 5	20 ± 5	20 ± 5	60 ± 5
Fuel Feed Method		Constant Level	Constant Level	Constant Level	Non-continuous fuel feed, allow to burn down	Constant Level	Constant Level
Oil Feed Mass	(kg)	268	256	243	221	243	230
Residue Mass	(kg)	31.5	28.4	32.9	39.7	29.3	19.6
Ratio (Residue/Feed)	(kg/kg)	0.12	0.11	0.14	0.18	0.12	0.09

7. SUMMARY

This report documents the sampling methods and analysis results of fuel characterization associated with 2-m pool fire testing of high-purity n-heptane, Bakken crude, and a diluted bitumen at Sandia National Laboratories for the National Research Council Canada.

Sampling and analysis methods were selected to be consistent with published industry standards and best practices. Basic physical and chemical properties were evaluated. Where available, measured values obtained here were compared to reference values, properties of similar oils, and equation of state model output.

High-level findings were as follows:

- 1) Heptane sample properties were consistent with high-purity (>99%) n-heptane and checked against the manufacturer statement of purity and NIST reference standard values
- 2) Bakken samples represented a light (43.9 °API), sweet (sulfur = 0.084 mass%) crude
 - a) Bakken VPCR_{0.2}(37.8°C) ranged from 120 kPa-152 kPa depending on sampling time and analysis laboratory
 - b) While some variations in sample-to-sample Bakken VPCR_x and composition were noted, these correlated strongly with laboratory and analytical methods, suggesting that method bias in sampling & analysis was more likely the cause than property changes of the base crude sample with time during sample storage
 - c) Calculated VPCR_x (37.8°C and 50°C) using whole oil composition passed through an EOS model compared well with measured VPCR_x by ASTM D6377-M
- 3) The diluted bitumen represented a heavy (21.7 °API), sour (sulfur = 3.6 mass%) crude
 - a) Dilbit VPCR_{0.2}(37.8°C) ranged from 86 kPa-94 kPa
 - b) A compositional analysis was consistent with a mixture of 20-25 vol% condensate (comprising C4-C8) and 75-80 vol% bitumen
 - c) Dilbit properties were stable with time across grab samples
 - d) Calculated VPCR_x (37.8°C and 50°C) using whole oil composition passed through an EOS model generally compared well with measured VPCR_x by ASTM D6377-M. Some method bias appeared in the T = 50°C comparison where EOS-modeled VPCR_x values were all around 10-15% lower than the measured values, but compared better at T = 37.8°C.

This page intentionally blank

8. REFERENCES

Alqaheem, S. S. and M. R. Riazi (2017). "Flash Points of Hydrocarbons and Petroleum Products: Prediction and Evaluation of Methods." *Energy & Fuels* **31**(4): 3578-3584.

Amani, M. J., M. R. Gray and J. M. Shaw (2014). "On correlating water solubility in ill-defined hydrocarbons." *Fuel* **134**: 644-658.

ANSI/API 2014 (Sep-2014) "Classifying and Loading of Crude Oil into Rail Tank Cars." **Recommended Practice 3000**. American Petroleum Institute, Washington, DC.

API (2011). "Crude Oil Category Assessment Document." High Production Volume Testing Group. American Petroleum Institute, Washington, DC 14-Jan-2011.

ASTM 2012 "Standard Practice for Manual Sampling of Petroleum and Petroleum Products." **ASTM D4057-12**. ASTM International, West Conshohocken, PA 19428-2959.

ASTM 2016a "Standard Test Method for Boiling Point Distribution of Samples with Residues Such as Crude Oils and Atmospheric and Vacuum Residues by High Temperature Gas Chromatography." **ASTM D7169-16**. ASTM International, West Conshohocken, PA 19429-2959.

ASTM 2013a "Standard Test Method for Density and Relative Density of Crude Oils by Digital Density Analyzer." **ASTM D5002-13**. ASTM International, West Conshohocken, PA 19428-2959.

ASTM 2011a "Standard Test Method for Density, Relative Density, and API Gravity of Liquids by Digital Density Meter." **ASTM D4052-11**. ASTM International, West Conshohocken, PA 19428-2959.

ASTM 2011b "Standard Test Method for Determination of Individual Components in Spark Ignition Engine Fuels by 100-Metre Capillary (with Precolumn) High-Resolution Gas Chromatography." **ASTM D6730-01 (Reapproved 2011)**. ASTM International, West Conshohocken, PA 19428-2959.

ASTM 2015 "Standard Test Method for Determination of Light Hydrocarbons and Cut Point Intervals in Live Crudes and Condensates by Gas Chromatography." **ASTM D8003-15**. ASTM International, West Conshohocken, PA 19428-2959.

ASTM 2016b "Standard Test Method for Determination of Vapor Pressure of Crude Oil: VPCRx(Expansion Method)." **ASTM D6377-16**. ASTM International, West Conshohocken, PA 19428-2959.

ASTM 2016c "Standard Test Method for Determination of Water in Petroleum Products, Lubricating Oils, and Additives by Coulometric Karl Fischer Titration." **ASTM D6304-11 (Reapproved 2016)**. ASTM International, West Conshohocken, PA 19428-2959.

ASTM 2016d "Standard Test Method for Flash Point by Tag Closed Cup Tester." **ASTM D56-16a**. ASTM International, West Conshohocken, PA 19429-2959.

ASTM 2014 "Standard Test Method for Heat of Combustion of Liquid Hydrocarbon Fuels by Bomb Calorimeter." **ASTM D240-14**. ASTM International, West Conshohocken, PA 19428-2959.

ASTM 2018 "Standard Test Method for Kinematic Viscosity of Transparent and Opaque Liquids (and Calculation of Dynamic Viscosity)." **ASTM D445-19**. ASTM International, West Conshohocken, PA 19428-2959.

ASTM 2016e "Standard Test Method for Sulfur in Petroleum and Petroleum products by Energy Dispersive X-Ray Fluorescence Spectrometry." **ASTM D4294-16**. ASTM International, West Conshohocken, PA 19428-2959.

ASTM 2016f "Standard Test Method for Water and Sediment in Crude Oil by the Centrifuge Methods (Laboratory Procedure)." **ASTM D4007-11 (Reapproved 2016)**. ASTM International, West Conshohocken, PA 19428-2959.

ASTM 2016g "Standard Test Method for Water in Organic Liquids by Coulometric Karl Fischer Titration." **ASTM E1064-16**. ASTM International, West Conshohocken, PA 19428-2959.

ASTM 2013b "Standard Test Methods for Flash Point by Pensky-Martens Closed Cup Tester." **ASTM D93-13**. ASTM International, West Conshohocken, PA 19429-2959.

ASTM 2016h "Standard Test Methods for Flash Point by Small Scale Closed Cup Tester." **ASTM D3828-16a**. ASTM International, West Conshohocken, PA 19428-2959.

Auers, J. R., R. M. Couture and D. L. Sutton (2014). "The North Dakota Petroleum Council Study on Bakken Crude Properties." Bakken Crude Characterization Task Force. North Dakota Petroleum Council, Bismarck, ND 58501. 4-Aug-2014.

Birn, K., J. Osuna, C. Velasquez, J. Meyer, S. Owens and M. Cairns (2014). "Crude by Rail: The new logistics of tight oil and oil sands growth." IHS Energy. https://ihsmarkit.com/pdf/IHS-Oil-Sands-Dialogue-Crude-by-rail-dec-2014_210390110913052132.pdf

Crudemonitor. (2019). from <https://crudemonitor.ca/>.

Enbridge Pipelines, I. and L. Enbridge Energy Partners (2012). 2012 Crude Characteristics. https://www.enbridge.com/~/media/Enb/Documents/Shippers/Crude_Characteristics_Booklet.pdf?la=en.

Enbridge Pipelines, I. and L. Enbridge Energy Partners (2018). 2018 Crude Characteristics. https://www.enbridge.com/~/media/Enb/Documents/Shippers/Crude_Characteristics_Booklet.pdf?la=en.

GPA 2014 "Obtaining Liquid Hydrocarbons Samples for Analysis by Gas Chromatography." **GPA 2174-14**. Gas Processors Association, Tulsa, OK 74145.

GPA 2003 "Tentative Method for the Analysis of Natural Gas Condensate Mixtures Containing Nitrogen and Carbon Dioxide by Gas Chromatography." **GPA Standard 2103-03**. Gas Processors Association, Tulsa, OK 74145.

Lord, D., R. Allen and D. Rudeen (2017). "DOE/DOT Crude Oil Characterization Research Study, Task 2 Test Report on Evaluating Crude Oil Sampling and Analysis Methods." **SAND2017-12482**. Sandia National Laboratories, Albuquerque, NM 87185. Nov-2017.

Lord, D., R. Allen, D. Rudeen, C. Wocken and T. Aulich (2018). "DOE/DOT Crude Oil Characterization Research Study, Task 2 Test Report on Evaluating Crude Oil Sampling and Analysis Methods, Revision 1 - Winter Sampling." **SAND2018-5909**. Sandia National Laboratories, Albuquerque, NM 87185. Jun-2018.

Luketa, A., T. K. Blanchat, D. L. Lord, A. Cruz-Cabrera, J. Hogge and R. Allen (2019). "Pool Fire and Fireball Experiments in Support of the US DOE/DOT/TC Crude Oil Characterization Research Study." **SAND 2019-9189**. Sandia National Laboratories, Albuquerque, NM USA 87185. August.

Luketa, A., A. Cruz-Cabrera, W. Gill, S. Ade and J. Hogge (2019). "Experimental Results of 2-m Heptane, Bakken Crude Oil, and Dilbit Pool Fire Tests Performed for the National Research Council Canada." **in press**. Sandia National Laboratories, Albuquerque, NM 87185.

PHMSA (2014). "Operation Safe Delivery Update." U.S. Department of Transportation, Washington, D.C. Jul-2014.

Prefontaine, A. (2015). "Final Report: Crude Oil Sampling and Analysis." Transport Dangerous Goods Directorate. Transport Canada. 10-Aug-2015. <https://www.tc.gc.ca/eng/tdg/safety-menu-1242.html>

Prefontaine, A. (2018). "Sample Plan: Collecting Samples from Modified 420 lb. Propane Tanks." Proprietary. InnoTech Alberta, Edmonton, AB, Canada. 07-Dec-2018.

Sagdeev, D. I., M. G. Fomina, G. K. Mukhamedzyanov and I. M. Abdulagatov (2013). "Experimental Study of the Density and Viscosity of n -Heptane at Temperatures from 298 K to 470 K and Pressure upto 245 MPa." *International Journal of Thermophysics* **34**(1): 1-33.

TC (2019). "Transportation of Dangerous Goods Regulations, Part 1." Government of Canada. **Transport Canada**. from <https://www.tc.gc.ca/eng/tdg/clear-part1-475.html#sec14>.

UOP 2010 "Hydrogen Sulfide and Mercaptan Sulfur in Liquid Hydrocarbons by Potentiometric Titration." **UOP 163**. ASTM International, West Conshohocken, PA 19428-2959.

Williamham, C. B., W. J. Taylor, J. M. Pignocco and F. D. Rossini (1945). "Vapor Pressures and Boiling Points of Some Paraffin, Alkylcyclopentane, Alkylcyclohexane, and Alkylbenzene Hydrocarbons." *J. Res. Nat. Bur. Stand. (U.S.)* **35**(3): 219-244.

APPENDIX A. DILBIT TANK FILL DATA

Sample Reference	Means of Containment	Sample Date	Sample Point	Start Time	End Time	Ambient Temperature (°C)	Barometric Pressure (hPa)	Sample Source Fluid Pressure (psi)	Sample Source Fluid Temperature (°C)	Volume Collected (L)	Comments
Day 1 Baseline samples											
FPC S/N 831453, CL7 Dilbit, Day 1 Baseline	Floating Piston Cylinder	28/Nov/18	Terminal	8:26	10:43	0	921	143	9.8	0.56	Baseline samples were collected directly from the source (pipeline) on each sampling day. These samples are being held at InnoTech Alberta in case further analysis is required.
Bottle #1 Day 1	1 L Boston Round Bottle	28/Nov/18	Terminal	8:26	10:43	0	921	143	9.8	1	
Bottle #1 Day 2	1 L Boston Round Bottle	28/Nov/18	Terminal							1	
Day 2 Baseline samples											
FPC S/N 830748, CL7 Dilbit, Day 2 Baseline	Floating Piston Cylinder	29/Nov/18	Terminal	8:05	10:46	-5	925	140	2.3	0.56	Baseline samples were collected directly from the source (pipeline) on each sampling day. These samples are being held at InnoTech Alberta in case further analysis is required.
Bottle #1 Day 1	1 L Boston Round Bottle	29/Nov/18	Terminal	8:05	10:46	-5	925	140	2.3	1	
Bottle #1 Day 2	1 L Boston Round Bottle	29/Nov/18	Terminal	8:05	10:46	-5	925	140	2.3	1	
Tank 5, CL7 dilbit	420 lb propane tank	28/Nov/18	Terminal	8:26	10:43	0	921	143	9.8	360	
Tank 6, CL7 Dilbit	420 lb propane tank	28/Nov/18	Terminal	8:26	10:43	0	921	143	9.8	360	
Tank 1, CL7 Dilbit	420 lb propane tank	28/Nov/18	Terminal	11:45	14:06	4.5	923	130	10.4	360	
Tank 2, CL7 Dilbit	420 lb propane tank	28/Nov/18	Terminal	11:45	14:06	4.5	923	130	10.4	360	
Tank 12, CL7 Dilbit	420 lb propane tank	28/Nov/18	Terminal	15:00	17:30	7.9	922	132	10.4	360	
Tank 8, CL7 Dilbit	420 lb propane tank	28/Nov/18	Terminal	15:00	17:30	7.9	922	132	10.4	360	
Tank 11, CL7 Dilbit	420 lb propane tank	29/Nov/18	Terminal	8:05	10:46	-5	925	140	2.3	360	
Tank 3, CL7 Dilbit	420 lb propane tank	29/Nov/18	Terminal	8:05	10:46	-5	925	140	2.3	360	
Tank 10, CL7 Dilbit	420 lb propane tank	29/Nov/18	Terminal	11:27	13:43	-1	931	140	5.2	360	
Tank 7, CL7 Dilbit	420 lb propane tank	29/Nov/18	Terminal	11:27	13:43	-1	931	140	5.2	360	
Tank 4, CL7 Dilbit	420 lb propane tank	29/Nov/18	Terminal	14:23	16:51	3	929.3	140	5.2	360	
Tank 9, CL7 Dilbit	420 lb propane tank	29/Nov/18	Terminal	14:23	16:51	3	929.3	140	5.2	360	

APPENDIX B. TABULAR LISTING OF VPCR_x DATA

B.1. Bakken VPCR_x Data

B.1.1. Direct measurements taken at 37.8 °C and 50 °C

Direct measurements																		
Label	B4-100-FPC-1- a-M	B4-100-FPC-1- b-M	B4-100-FPC-2- a-M	B4-100-FPC-2- b-M	B4-100-FPC-3- a-M	B4-100-FPC-3- b-M	B4-122-FPC-1- a-M	B4-122-FPC-1- b-M	B6-100-FPC-1- a-M	B6-100-FPC-1- b-M	B6-100-FPC-2- a-M	B6-100-FPC-2- b-M	B6-100-FPC-2- c-M	B6-100-FPC-2- d-M	B6-122-FPC-1- a-M	B6-122-FPC-1- b-M		
Event Abbreviation	B4	B6	B6															
Sampling Date	1/18/2018	1/18/2018	1/18/2018	1/18/2018	1/18/2018	1/18/2018	1/18/2018	1/18/2018	1/31/2018	1/31/2018	1/31/2018	1/31/2018	1/31/2018	1/31/2018	1/31/2018	1/31/2018	1/31/2018	
Temperature	100	100	100	100	100	100	122	122	100	100	100	100	100	100	122	122	122	
Sample Container	FPC	FPC																
Cylinder Replicate	1	1	2	2	3	3	1	1	1	1	2	2	2	2	1	1	1	
Repeatability Replicate	a	b	a	b	a	b	a	b	a	b	a	b	c	d	a	b		
Sampling Temperature (F)																		
Sampling Pressure (psig)																		
Measured/Simulated	M	M	M	M	M	M	M	M	M	M	M	M	M	M	M	M	M	
VPCR _x (at these V/L)	0.0																	
	0.05																	
	0.1																	
	0.2	20.00	19.99	19.97	19.97	19.93	19.93	24.03	24.03	22.66	22.64	21.86	21.84	21.03	21.03	25.09	25.06	
	0.5	16.62	16.62	17.01	17.03	16.80	16.84	20.73	20.74	18.42	18.46	17.87	17.85	17.54	17.54	21.51	21.52	
	1.0	14.68	14.69	15.19	15.19	14.74	14.74	18.57	18.55	15.88	15.87	15.56	15.56	14.98	14.99	19.03	19.03	
	1.5	13.63	13.63	13.98	13.98	13.67	13.66	17.22	17.23	14.26	14.26	14.17	14.17	13.75	13.72	17.41	17.61	
	2.0	12.84	12.84	13.10	13.11	12.88	12.89	16.36	16.38	13.42	13.40	13.27	13.29	12.93	12.92	16.71	16.72	
	4.0	11.04	11.05	11.17	11.18	10.99	10.99	13.92	13.94	11.21	11.20	11.21	11.21	11.01	11.01	14.26	14.24	

B.1.2. Summary of measurements on shared Bakken samples from Luketa, Blanchat et al. (2019)

	Label	B1-100-FPC-1– B1-100-FPC-2– B2-100-FPC-1– B2-100-FPC-1– B2-100-FPC-2– B6-100-MPC– B6-100-MPC– B6-100-MPC– B8-100-MPC– B8-100-MPC– B8-100-MPC– B8-100-MPC–	M	M	a-M	b-M	M	1-a-M	1-b-M	2-a-M	2-b-M	1-a-M	1-b-M	2-a-M	2-b-M
	Event Abbreviation	B1	B1	B2	B2	B2	B6	B6	B6	B6	B6	B8	B8	B8	B8
Sampling Date	8/17/2017	8/17/2017	10/2/2017	10/2/2017	10/2/2017	7/18/2018	7/18/2018	7/18/2018	7/18/2018	10/4/2018	10/4/2018	10/4/2018	10/4/2018	10/4/2018	10/4/2018
Temperature	100	100	100	100	100	100	100	100	100	100	100	100	100	100	100
Sample Container	FPC	FPC	FPC	FPC	FPC	MPC									
Cylinder Replicate	1	2	1	1	2	1	1	2	2	1	1	2	2	2	2
Repeatability Replicate			a	b		a	b	a	b	a	b	a	b	a	b
Sampling Temperature (F)	75		70	70	70										
Sampling Pressure (psig)	148		45	45	45										
Measured/Simulated	M	M	M	M	M	M	M	M	M	M	M	M	M	M	M
VPCRx (at these V/L)	0.0														
	0.05	18.53	18.10	27.71	28.00	26.61	22.64	23.56	20.75	21.49					
	0.1		17.40	19.78	19.95	21.50	22.33	22.32	19.66	19.82	19.18	18.99	19.02	19.01	
	0.2	17.83	17.07	19.18	19.15	19.42	20.11	20.08	18.60	18.31	18.15	18.10	17.79	18.05	
	0.5	15.70	15.40	16.09	16.04	16.21	16.23	16.56	15.22	15.37	15.25	15.25	15.30	15.40	
	1.0														
	1.5		12.79	13.16	13.08	12.96	13.06	13.03	12.53	12.34	12.40	12.37	12.25	12.40	
	2.0														
	4.0		9.87	10.61	10.18	10.23	10.18	10.10	10.38	9.54	9.58	9.58	9.68	9.58	9.65

B.1.3. Values calculated from process simulator

	Label	B1-100-FPC-1– B1-100-FPC-2– B1-122-FPC-1– B1-122-FPC-2– B2-100-FPC-2– B2-122-FPC-2– B4-100-FPC-1– B4-122-FPC-1– B4-100-FPC-2– B4-122-FPC-2– B6-100-FPC-1– B6-122-FPC-1– B6-100-FPC-2– B6-122-FPC-2– B8-100-WD-4– B8-122-WD-4–	U	U	U	U	U	U	U	U	U	U	U	U	U	U
	Event Abbreviation	B1	B1	B1	B1	B2	B2	B4	B4	B4	B4	B6	B6	B6	B6	
Sampling Date	8/17/2017	8/17/2017	8/17/2017	8/17/2017	10/2/2017	10/2/2017	1/18/2018	1/18/2018	1/18/2018	1/31/2018	1/31/2018	1/31/2018	1/31/2018	1/31/2018	7/18/2018	
Temperature	100	100	122	122	100	122	100	122	100	122	100	122	100	122	100	
Sample Container	FPC	FPC	FPC	FPC	FPC	FPC	FPC	FPC	FPC	FPC	FPC	FPC	FPC	FPC	WD	
Cylinder Replicate	1	2	1	2	2	2	1	1	2	1	1	2	2	2	4	
Repeatability Replicate																
Sampling Temperature (F)																
Sampling Pressure (psig)																
Measured/Simulated	U	U	U	U	U	U	U	U	U	U	U	U	U	U	U	
VPCRx (at these V/L)	0.0	192.16	148.17	223.40	178.28	152.31	181.00	143.14	171.49	150.17	178.54	198.51	222.42	167.18	195.51	
	0.05	177.41	140.04	208.41	169.99	142.45	170.97	139.42	162.88	140.46	168.77	175.78	205.04	153.95	182.19	
	0.1	166.79	134.11	197.44	163.80	135.21	163.57	134.66	156.54	133.45	161.57	163.53	192.63	144.59	172.61	
	0.2	152.10	125.76	182.13	154.93	125.35	153.15	120.04	147.57	123.79	151.46	147.20	175.82	131.99	159.50	
	0.5	129.35	112.11	157.52	139.73	109.63	136.09	106.53	132.65	108.64	134.99	123.21	150.33	113.05	139.10	
	1.0	111.99	100.67	137.96	126.28	97.39	122.00	95.51	119.85	96.83	121.43	106.24	131.39	99.04	123.18	
	1.5	102.18	93.63	126.51	117.67	90.19	113.41	88.95	111.76	89.92	113.15	97.06	120.69	91.14	113.81	
	2.0	95.41	88.43	118.37	111.19	85.06	107.12	84.03	105.71	84.96	107.07	90.79	113.17	85.60	107.06	
	4.0	79.36	75.22	98.66	94.42	72.40	91.23	71.71	90.03	72.65	91.54	76.06	94.97	72.18	90.28	

B.2. Dilbit VPCRx Data

B.2.1. Direct measurements taken at 37.8 and 50°C

Direct measurements		D1-100-FPC-1- a-M	D1-100-FPC-1- b-M	D1-122-FPC-1- a-M	D1-122-FPC-1- b-M	D2-100-FPC-1- a-M	D2-100-FPC-1- b-M	D2-122-FPC-1- a-M	D2-122-FPC-1- b-M	D4-100-FPC-1- a-M	D4-100-FPC-1- b-M	D4-122-FPC-1- a-M	D4-122-FPC-1- b-M
	Label	D1	D1	D1	D1	D2	D2	D2	D2	D4	D4	D4	D4
Event Abbreviation		D1	D1	D1	D1	D2	D2	D2	D2	D4	D4	D4	D4
Sampling Date		11/28/2018	11/28/2018	11/28/2018	11/28/2018	12/3/2018	12/3/2018	12/3/2018	12/3/2018	1/28/2019	1/28/2019	1/28/2019	1/28/2019
Temperature		100	100	122	122	100	100	122	122	100	100	122	122
Sample Container		FPC											
Cylinder Replicate		1	1	1	1	1	1	1	1	1	1	1	1
Repeatability Replicate		a	b	a	b	a	b	a	b	a	b	a	b
Sampling Temperature (F)													
Sampling Pressure (psig)													
Measured/Simulated		M	M	M	M	M	M	M	M	M	M	M	M
VPCRx (at these V/L)	0.0												
	0.05	117.10	116.60	141.20	141.20	143.60	143.70	194.30	194.40				
	0.1	91.20	90.70	123.30	123.30	115.70	115.40	145.40	145.40				
	0.2	85.80	85.60	116.30	116.30	98.10	98.10	134.50	134.70	94.40	94.30	129.80	129.60
	0.5	74.70	74.70	104.40	104.40	81.50	81.40	112.60	112.40	79.70	79.50	109.30	109.20
	1.0	67.90	64.70	95.50	95.70	69.80	69.50	97.20	97.30	68.90	68.90	96.60	96.60
	1.5	64.40	64.50	92.10	92.00	66.00	66.00	93.90	93.90	64.90	65.00	92.20	91.80
	2.0	61.50	61.60	86.40	86.80	61.10	61.50	88.40	89.30	62.40	62.30	88.70	88.70
	4.0	55.30	55.30	78.10	78.20	56.20	56.20	81.60	81.60	54.90	54.90	81.40	81.50

B.2.2. Values calculated from process simulator

Values calculated from process simulator						
	Label	D1-100-FPC-1- D1-122-FPC-1- D2-100-FPC-1- D2-122-FPC-1- D4-100-FPC-1- D4-122-FPC-1-	U	U	U	U
Event Abbreviation	D1	D1	D2	D2	D4	D4
Sampling Date	11/28/2018	11/28/2018	12/3/2018	12/3/2018	1/28/2019	1/28/2019
Temperature	100	122	100	122	100	122
Sample Container	FPC	FPC	FPC	FPC	FPC	FPC
Cylinder Replicate	1	1	1	1	1	1
Repeatability Replicate						
Sampling Temperature (F)						
Sampling Pressure (psig)						
Measured/Simulated	U	U	U	U	U	U
0.0	99.58	122.23	144.15	167.76	114.44	137.35
0.05	91.55	114.10	127.25	150.86	103.36	126.24
0.1	86.06	108.47	115.95	139.46	95.90	118.68
0.2	78.92	101.07	101.66	124.90	86.39	108.90
0.5	68.78	90.29	82.51	105.01	73.34	95.20
1.0	62.00	82.77	70.79	92.45	65.02	86.10
1.5	58.56	78.75	65.32	86.35	60.95	81.43
2.0	56.31	76.00	61.96	82.45	58.35	78.31
4.0	51.22	69.33	55.01	73.83	52.65	70.98

APPENDIX C. TABULAR LISTING OF COMPOSITIONAL DATA

C.1. *n*-Heptane Compositional Data

n-Heptane manufacturer certificate of analysis

		
Certificate of Analysis		
N-HEPTANE, HIGH PURITY		
Lot/Batch #:	C17H29DRM-000HP99	
Customer PO #:	00001	
Parchem Order #:	33008	
Test	Limit	Result
Assay (as <i>n</i> -Heptane)	≥ 99.0%	99.45%
Assay (as C7 Hydrocarbons)	≥ 99.5%	99.98%
Assay (Total Hydrocarbons)	≥ 99.9%	99.98%
Specific Gravity (15.56°C)	0.680 – 0.695	0.689
Titrable Acid	≤ 0.0003 meq/g	< 0.003 meq/g
Residue after Evaporation	≤ 10 ppm	0 ppm
Sulfur Compounds (as S)	≤ 0.005%	0.000%
Water	≤ 0.03%	< 0.01%

QA Review: 

QA Approval: 


parchem – fine & specialty chemicals | 415 Huguenot Street, New Rochelle, NY 10801 | Tel: 914-654-6800 | www.parchem.com | dox@parchem.com
Form #: 2343 Date: 1.20.12 Revision: 10 Revision Date: 12.2.2016

n-Heptane analytical laboratory report of analysis

Sample ID:	2018-NOLA-000177-010	Date Taken:	8-Jan-18
Sample Designated As:	HEPTANE	Date Submitted:	8-Jan-18
Vessel/Location:	TTC SANDIA HEPTANE	Date Tested:	11-Jan-18
Representing:	TTC SANDIA HEPTANE Equal Composite		
Method	Test	Result	Unit
ASTM D4052	API Gravity @ 60°F	74.1	°API
ASTM D4052	Density @ 15.56°C	0.6875	g/cm³
ASTM D4052	Relative Density, 15.56°C/15.56°C	0.6882	
ASTM D6730	Ignition Fuels by 100-m GC	See Attached Report	
ASTM D6730	Heptane Purity	99.5	Vol %
ASTM D240	Gross Heat of Combustion	20558	BTU/lb
ASTM E1064	Water Content	25	mg/kg
ASTM D93	Procedure Used	A	
ASTM D93	Corrected Flash Point	<50	°F
ASTM D3828	Procedure Used	A	
ASTM D3828	Flash/No Flash	Flash	
ASTM D3828	Target Flash Point	-5	°F
LWI_ELDF_007_001	Average Molecular Weight	102.14	g/mol

¹ Outside Scope of Method

² Outside Laboratory

C.2. Bakken Compositional Data and Whole Oil Properties

		Bakken							
Label		B1-FPC-1	B1-FPC-2	B2-FPC-3	B4-1	B4-2	B6-1	B6-2	B8-WD-4
Event Abbreviation		B1	B1	B2	B4	B4	B6	B6	B8
Sampling Date		8/17/2017	8/17/2017	10/2/2017	1/18/2018	1/18/2018	1/31/2018	1/31/2018	7/18/2018
Sample Container		FPC	FPC	FPC					WD
Event Replicate		1	2	3	1	2	1	2	4
Composition (mol%)	CO2	0.0260	0.0070	0.0070	0.0018	0.0000	0.0015	0.0012	0.0040
	CO				0.0000	0.0000	0.0000	0.0000	
	H2S				0.0000	0.0000	0.0000	0.0000	
	He				0.0000	0.0000	0.0000	0.0000	
	H2				0.0002	0.0000	0.0000	0.0000	
	O2				0.0038	0.0013	0.0169	0.0025	
	N2	0.1150	0.0610	0.0770	0.0662	0.0756	0.1540	0.1101	0.1900
	C1	0.1100	0.0590	0.0580	0.0469	0.0524	0.0475	0.0496	0.0580
	C2	0.6350	0.6300	0.5470	0.5441	0.5460	0.5569	0.5398	0.5300
	C3	2.7560	2.7370	2.5570	2.6734	2.6442	2.7427	2.6453	2.5660
	iC4	1.0110	0.9560	0.9080	0.9522	0.9366	0.9733	0.9350	0.9120
	nC4	4.8920	4.7840	4.5760	4.7931	4.7295	4.9279	4.7297	4.5660
	neo C5				0.0097	0.0000	0.0000	0.0000	
	iC5	2.3390	2.2520	2.1600	2.2594	2.2321	2.3082	2.2295	2.1680
	nC5	4.5910	4.5260	4.3500	4.5298	4.4741	4.6407	4.4715	4.3390
	C6	5.83	6.54	7.83	7.17	7.08	7.31	7.06	6.65
	Benzene	0.43	0.50	0.64	0.45	0.43	0.46	0.42	0.47
	C7	12.80	13.35	15.12	10.54	10.41	10.72	10.36	13.47
	C8	14.51	14.35	15.31	11.50	11.36	11.68	11.30	14.33
	C9	7.91	7.16	7.35	8.09	8.01	8.10	7.94	7.17
	C10	6.10	6.17	5.88	6.81	7.51	6.72	7.43	6.31
	C11	4.69	4.74	4.46	5.09	4.75	5.05	4.68	4.85
	C12	3.85	3.86	3.60	4.35	4.34	4.32	4.37	3.96
	C13	3.47	3.48	3.28	3.81	3.90	3.79	3.84	3.60
	C14	2.94	2.95	2.76	3.34	3.42	3.33	3.45	3.02
	C15	2.49	2.50	2.32	2.69	2.76	2.68	2.70	2.55
	C16	2.12	2.10	1.96	2.20	2.19	2.13	2.21	2.16
	C17	1.81	1.81	1.68	2.13	2.19	2.20	2.14	1.86
	C18	1.59	1.58	1.47	1.69	1.75	1.64	1.76	1.62
	C19	1.43	1.43	1.31	1.36	1.36	1.38	1.37	1.46
	C20	1.24	1.23	1.15	1.24	1.30	1.26	1.25	1.26
	C21	1.08	1.08	0.99	1.17	1.23	1.14	1.24	1.10
	C22	0.97	0.96	0.88	1.01	1.01	0.98	1.02	0.98
	C23	0.84	0.83	0.76	0.87	0.92	0.94	0.93	0.85
	C24	0.74	0.73	0.67	0.84	0.83	0.81	0.84	0.74
	C25	0.66	0.66	0.61	7.85	7.57	6.97	7.96	6.25
	C26	0.61	0.59	0.54					
	C27	0.54	0.54	0.50					
	C28	0.49	0.48	0.43					
	C29	0.44	0.44	0.38					
	C30+	3.96	3.93	2.86					

Label	Bakken							
	B1-FPC-1	B1-FPC-2	B2-FPC-3	B4--1	B4--2	B6--1	B6--2	B8-WD-4
Event Abbreviation	B1	B1	B2	B4	B4	B6	B6	B8
Sampling Date	8/17/2017	8/17/2017	10/2/2017	1/18/2018	1/18/2018	1/31/2018	1/31/2018	7/18/2018
Sample Container	FPC	FPC	FPC					WD
Event Replicate	1	2	3	1	2	1	2	4
IBP, °C (ASTM D86)				32.90	32.90	27.30	27.30	
Flash Pt-closed cup, °C (ASTM D3828)				<-30	<-30	<-30	<-30	
Sediment, % (ASTM D4007)				0.03	0.03	0.03	0.03	
Water, % (ASTM D4007)				0.00	0.00	0.12	0.12	
Water+Sediment, % (ASTM D4007)				0.03	0.03	0.15	0.15	
Water, mass% (Karl Fischer)				0.01	0.01	0.16	0.16	
Density @ 15 °C, kg/m^3 (ASTM D5002)				809.60	809.60	810.00	810.00	
Heat of Combustion, MJ/kg (ASTM D240)				46.02	46.02	45.97	45.97	
Sulfur, mass% (ASTM D4294)								
Viscosity, cSt (ASTM D445)								
H2S, ppm (UOP 163)								
Mercaptans, ppm (UOP 163)								
Specific Gravity at 60°F	0.80	0.80	0.80					0.80
API Gravity at 60°F	44.54	44.84	45.18					44.67
Molecular Weight	160.55	156.56	153.83					156.30
Pounds per Gallon (in Vacuum)	6.70	6.69	6.68					6.70
Pounds per Gallon (in Air)	6.69	6.68	6.67					6.69
Cu. Ft. Vapor per Gallon @ 14.696 psia	15.84	16.22	16.47					16.26
Specific Gravity at 60°F	0.94	0.94	0.95					0.95
API Gravity at 60°F	18.66	18.50	17.30					18.17
Molecular Weight	548.66	550.07	537.56					544.56
Pounds per Gallon (in Vacuum)	7.86	7.87	7.93					7.88
Pounds per Gallon (in Air)	7.85	7.86	7.92					7.87
Cu. Ft. Vapor per Gallon @ 14.696 psia	5.43	5.43	5.60					5.49
Shrinkage Factor	0.99	0.99	0.99					0.99
Flash Factor, Cu.Ft./STBbl.	2.11	7.10	15.27					5.74
Simulated Flash Factor (69F)	2.30	0.50						
Color Visual	Straw	Straw	Straw					Dark Amber
API Gravity @ 60° F	42.52	42.55	42.76					42.51
< C6 mass%	6.17	6.17	5.99	5.91	5.84	6.22	5.80	5.91

C.3. Dilbit Compositional Data and Whole Oil Properties

		Dilbit		
		D1-FPC-1	D2-FPC-1	D4-FPC-1
		D1	D2	D4
		12/3/2018	1/28/2019	2/27/2019
		FPC	FPC	FPC
	Event Replicate	1	1	1
	CO2	0.0220	0.0183	0.0230
	CO	0.0000	0.0000	
	H2S	0.0000	0.0000	
	He	0.0000	0.0000	
Composition (mol%)	H2	0.0000	0.0000	
	O2	0.0000	0.0127	
	N2	0.0606	0.1375	0.0915
	C1	0.0649	0.0504	0.0498
	C2	0.0382	0.0417	0.0430
	C3	0.3601	0.3962	0.4125
	iC4	0.7012	0.7416	0.7538
	nC4	2.6936	2.9511	2.9819
	neo C5	0.1803	0.0689	0.0646
	iC5	8.9704	9.1680	8.8073
	nC5	9.8367	9.9882	9.6282
	C6	8.34	8.60	8.40
	Benzene	0.45	0.47	0.47
	C7	6.23	6.55	6.51
	C8	5.29	5.53	5.62
	C9	2.70	3.04	3.11
	C10	2.16	1.76	2.15
	C11	1.49	1.45	1.77
	C12	1.66	1.62	1.76
	C13	1.80	1.76	1.75
	C14	1.92	1.88	1.99
	C15	1.65	1.61	1.72
	C16	1.64	1.60	1.70
	C17	1.95	1.90	1.89
	C18	1.74	1.61	1.79
	C19	1.48	1.45	1.53
	C20	1.41	1.47	1.46
	C21	1.50	1.47	1.54
	C22	1.35	1.32	1.32
	C23	1.30	1.20	1.26
	C24	1.10	1.15	1.14
	C25	30.00	28.98	28.25
	C26			
	C27			
	C28			
	C29			
	C30+			

		Dilbit		
Label		D1-FPC-1	D2-FPC-1	D4-FPC-1
Event Abbreviation		D1	D2	D4
Sampling Date	12/3/2018	1/28/2019	2/27/2019	
Sample Container	FPC	FPC	FPC	
Event Replicate	1	1	1	
IBP, °C (ASTM D86)	33.30	33.60	34.00	
Flash Pt-closed cup, °C (ASTM D3828)	<-30.0	<-30.0	<-30.0	
Sediment, % (ASTM D4007)	0.05	<0.025	0.03	
Water, % (ASTM D4007)	0.45	0.20	0.28	
Water+Sediment, % (ASTM D4007)	0.50	0.20	0.30	
Water, mass% (Karl Fischer)	0.75	0.51	0.56	
Density @ 15 °C, kg/m^3 (ASTM D5002)	923.50	924.20	923.90	
Heat of Combustion, MJ/kg (ASTM D240)	42.84	43.28	43.41	
Sulfur, mass% (ASTM D4294)	3.68	3.65	3.42	
Viscosity, cSt (ASTM D445)	76.41	70.26	68.99	
H2S, ppm (UOP 163)	6.30	0.50	2.00	
Mercaptans, ppm (UOP 163)	113.60	99.60	120.00	
Specific Gravity at 60°F				
API Gravity at 60°F				
Molecular Weight				
Pounds per Gallon (in Vacuum)				
Pounds per Gallon (in Air)				
Cu. Ft. Vapor per Gallon @ 14.696 psia				
Specific Gravity at 60°F				
API Gravity at 60°F				
Molecular Weight				
Pounds per Gallon (in Vacuum)				
Pounds per Gallon (in Air)				
Cu. Ft. Vapor per Gallon @ 14.696 psia				
Shrinkage Factor				
Flash Factor, Cu.Ft./STBbl.				
Simulated Flash Factor (69F)				
Color Visual				
API Gravity @ 60° F				
< C6 mass%	6.54	6.85	6.67	

DISTRIBUTION

Email—External [REDACTED]

Name	Company Email Address	Company Name
Yoon Ko	Yoon.Ko@nrc-cnrc.gc.ca	National Research Council Canada
Celia Lam	Celia.Lam@nrc-cnrc.gc.ca	National Research Council Canada

Email—Internal

Name	Org.	Sandia Email Address
Anay Luketa	01532	aluketa@sandia.gov
Technical Library	01177	libref@sandia.gov

This page left blank

This page left blank



**Sandia
National
Laboratories**

Sandia National Laboratories is a multimission laboratory managed and operated by National Technology & Engineering Solutions of Sandia LLC, a wholly owned subsidiary of Honeywell International Inc. for the U.S. Department of Energy's National Nuclear Security Administration under contract DE-NA0003525.